Hydrophobic and hydrophilic balance of biodegradable poly(thio ketal) polymers and their use as antioxidant systems for tissue regeneration

By

Katherine Russo

Thesis

Submitted to the Faculty of the
Graduate School of Vanderbilt University
in partial fulfillment of the requirements for
the degree of

MASTER OF SCIENCE

in

Biomedical Engineering
May 14, 2021

Nashville, TN

Approved:

Craig L. Duvall, Ph.D.
Scott A. Guelcher, Ph.D.

ACKNOWLEDGEMENTS

Throughout this research experience and writing of this thesis, I have received a great deal of support. I would first like to thank my research advisor, Dr. Craig Duvall, who accepted me into the Advanced Therapeutics Laboratory and provided valuable expertise in designing experiments and protocols. Your helpful feedback has pushed me to bring my work to a higher level.

I would like to acknowledge my fellow lab members and colleagues, whose support and expertise in helped a tremendously in formulating research questions and learning techniques and instruments.

In addition, I would like to thank my parents and sister for being an endless mode of support during this process. Their advocation and encouragement was a constant during this project. Finally, I would like to thank my friends and boyfriend, Jake, for supporting me and encouraging me to produce my best work.

Table of Contents

List of Tables

List of Figures

List of Equations

CHAPTER I: Introduction and significance

1.1 Motivation

Chronic wounds, such as diabetic foot ulcers, pressure ulcers, and venous ulcers, are wounds that are unable to heal properly on their own and often are associated with a pathologic state of inflammation[1]. This not only poses risk for infection, but also causes pain and distress to the patient[2]. Additionally, these non-healing wounds have shown to drain the healthcare system of money and resources[2]. Foot ulcers are among the most common of chronic wounds, affecting an estimated 6.5 million people every year, with expenses amounting to $25 billion per year in the United States[2]. One of the most common types of chronic wounds is the diabetic foot ulcer, which is caused in part by the disruption of oxygen homeostasis, leading to a cascade effect impairing growth factor production, angiogenesis, and granulation tissue formation[3]. The purpose of this project is to test a stimuli-responsive scaffold for the tunable, carrier-free release of a biological therapeutic to promote the production of growth factors, tissue infiltration, and angiogenesis in chronic wounds. In subsequent future work, the foam scaffold will be loaded with both free and covalently bonded drug, and the tunable degradation of the scaffold will lead to subsequent release of the therapeutic.

1.2 Innovation

PTK-UR biomaterials are one of the first synthetic tissue engineering materials to have exclusively cell-mediated degradation via cell-produced reactive oxygen species[4]. Additionally, the presented biodegradable biomaterial is one of the first reported hydrophilic PTK materials, which acts to improve degradation kinetics and antioxidant

capacity of the system. They sustain long-term ROS-mediated degradation with the absence of hydrolytic degradation in an aqueous environment. Along with ROS-dependent degradation, thioketal bonds act as antioxidant scavengers to reduce environmental oxidants and provide cells with protection from oxidative environments, with greater bond exposure with increased hydrophilicity.

1.3 Specific Aims

The central hypothesis of this project is that as the hydrophilicity of the biodegradable PTK-UR polymeric scaffolds increases, the ability to scavenge free radicals will increase and the degradation kinetics via reactive oxygen species accelerate, allowing for enhanced cell growth and modulation of cell behavior in a chronic wound environment.

Aim 1: Understand how hydrophobic/hydrophilic balance affects material and degradation properties of PTK-UR scaffolds

The first aim of this thesis is to understand how the chemical composition and material properties of a library of poly(thio ketal urethane) (PTK-UR) scaffolds varies with hydrophilic/hydrophobic balance. The library of scaffolds is synthesized from PTK diols with deionized water, TEGOAMIN33, calcium stearate, and Lysine Triisocyanate (LTI) via liquid reactive molding. Objective 1 is to analyze the physical properties of the PTK-UR scaffold library, and objective 2 is to determine the hydrophilic/hydrophobic gradient of the PTK-UR scaffolds with varying polyethylene glycol (PEG) content within the monomer, how this balance affects scaffold mechanics, and ROS-mediated degradation of scaffolds.

2

To verify chemical composition of the polymer diols as outlined in objective 1, Differential Scanning Calorimetry (DSC) was used to determine the glass transition temperatures (T_g) of each of the diols in the polymer library. Soluble fraction of formulated scaffolds identifies the fraction of polyol that is crosslinked with the isocyanate during the formulation process, while core porosity and crosslink density quantifies the degree of porosity and degree of crosslinking in scaffolds, respectively.

For objective 2, contact angle on polymer films and swell ratio of PTK-UR scaffolds were used to measure the hydrophilicity of scaffolds, with the hypothesis that the diols increase in hydrophilicity with increasing PEG content within the diol. Mechanical properties, (Young's Modulus) was measured via dynamic mechanical analysis (DMA) for both dry and wet scaffolds. Degradation properties were evaluated via incubation in hydrogen peroxide (H_2O_2) with cobalt chloride ($CoCl_2$) for ROS-mediated breakdown of the scaffolds, specifically via hydroxyl radicals. Mass loss over time and subsequent swell ratio were recorded over time during ROS exposure. Mass loss data was fitted to a first order degradation model using MATLAB, and this model was used to determine degradation rate constants for each scaffold in oxidative media. Scanning electron microscopy (SEM) was used to evaluate the change in pore structure following exposure to the ROS-containing media.

Aim 2: Measure ability of PTK-UR scaffolds to harbor cell growth and protect against ROS mediated toxicity

The second aim of this project is to determine how biodegradable poly(thio ketal) biomaterials with varying hydrophilicities modulate cell growth and cell function. Objective 1 is to measure cell cytocompatibility with PTK materials, and objective 2 is to determine the antioxidant capacity and cell protection ability of PTK-UR scaffolds in oxidative environments.

Cytocompatibility was confirmed by measuring cell viability of NIH 3T3 mouse fibroblast cells cultured by seeding cells onto a 96-well plate and treating with extracts from the PTK-UR scaffolds. Cell viability was measured via bioluminescence in comparison to no treatment controls. The 1,1-diphenyl-2-picrylhydrazyl (DPPH) assay was used to analyze and quantify antioxidant capacity of PTK-UR scaffolds in 80% ethanol/water, and radical reduction was measured over time via absorbance measurement of test solutions. Cell protection from oxidative environment was evaluated by treating NIH 3T3 mouse fibroblast cells with hydrogen peroxide-containing media and crudely solubilized diols to act as ROS-scavengers. Luminescence was used to measure cell viability via CellTiter-Glo luminescent assay.

1.4 Outline

This thesis describes the *in vitro* material characterization of a ROS-scavenging tissue engineering scaffold system and how it can be used to control cellular behavior in oxidative environments. Chapter 2 will provide a review of wound and chronic wound pathology, as well as biomaterial-based treatment approaches for such pathologies.

Chapter 3 will discuss the analysis of physical properties of the PTK polymers and scaffolds, as well as the hydrophilic/hydrophobic balance of the library of polymers and associated degradation properties in comparison to conventional polyester urethane (PEUR) materials. Chapter 4 will detail the *in vitro* biocompatibility and modulation of cell function of the library of PTK-UR scaffolds compared to PEUR controls. Finally, chapter 5 will contain a summary that describes broader impacts, current challenges, and future directions of this class of biomaterials. Each of the experimental chapters will contain a concise introduction and methods section with respective results and discussion.

CHAPTER 2: Background

2.1 Wound Healing

The skin is a complex tissue that serves as a barrier between the body and the environment. Upon injury, it must be repaired in an effective manner in order to maintain its function for the body. Wound healing occurs in four phases: hemostasis, inflammation, proliferation, and tissue remodeling, and the process can take up to one year to be completed depending on the severity of the wound[1,5,6]. Throughout this process, there are multiple factors that help or hinder the progression to the next phase of healing, including cell recruitment, growth factor production, cytokine and chemokine production, and hypoxia and ischemia[3,5]. Issues associated with any of these factors can lead to the inability for the healing phases to progress correctly. In some cases, this can lead to the development of chronic wounds.

2.1.1 Phases of Wound Healing

The first phase of wound healing is hemostasis. This phase involves the coagulation of platelets that release biochemical mediators that work to minimize blood loss by causing vasoconstriction[1,5]. As the platelets interact with the injury, they release thrombin which converts to fibrin to form a fibrin clot and stop the bleeding[1,5,6]. As the platelets de-granulate, they release cytokines and growth factors such as transforming growth factor (TGF)-β, platelet-derived growth factor (PDGF), fibroblast growth factor (FGF), and epidermal growth factor (EGF)[1,5,6]. These factors attract both inflammatory and non-inflammatory cells that are involved in the subsequent phases of wound healing. The inflammatory phase begins when these cells migrate to the wound site.

Inflammation is the second phase of wound healing, which begins moments after injury and can last days to weeks[5]. The main purpose of this phase is to establish a barrier to eliminate the invasion of microorganisms and other foreign materials into the wound[7]. Neutrophils are the first cell to arrive, and remove bacteria and other materials from the site of the wound via phagocytosis[8]. Once bacteria and other debris have been removed from the wound site, neutrophil activity decreases and they are gradually eliminated. Meditators and cytokines released during neutrophil activity act as a chemoattractant for monocytes, which eventually undergo a phenotypic change into M1 macrophages[5,7,9]. M1 macrophages are pro-inflammatory and further eliminate pathogens and remove damaged tissue from the wound site[9]. They also rid the wound of apoptotic neutrophils, which promotes the differentiation into anti-inflammatory macrophages (M2) that drive the resolution of the inflammatory phase[6]. Macrophages in the wound also secrete chemical messengers to activate the infiltration, migration, and proliferation of keratinocytes, fibroblasts, and endothelial cells[5,7].

The third phase involved in wound healing is proliferation. In this phase, cells that have infiltrated the wound area, including fibroblasts, endothelial cells, and epithelial cells, rapidly begin to divide and migrate to develop the initial scar tissue[5]. Fibroblasts migrate and proliferate in the wound, depositing matrix proteins hyaluronan, fibronectin, proteoglycans, and type 1 and type 3 procollagen, replacing the temporary fibrin matrix[5–7]. As this ECM further accumulates, fibroblasts transition into myofibroblasts, which begin wound contraction[5,7]. Concurrently with these processes, vascular networks are repaired in the wound. Endothelial cells are activated by a number of angiogenic factors, resulting in a cascade of events that lead to vessel formation. Epithelialization also

occurs, in which epithelial cells and keratinocytes begin to reform the barrier function of the skin. This process promotes the production of new extracellular matrix, as well as growth factor and cytokine expression[5,6]. The establishment of a new stratified epidermis begins when a monolayer of keratinocytes covers the wound site, and differentiation and stratification replaces the proliferative and migratory activities occurring at the injury[5]. This begins the formation of the basement membrane[7].
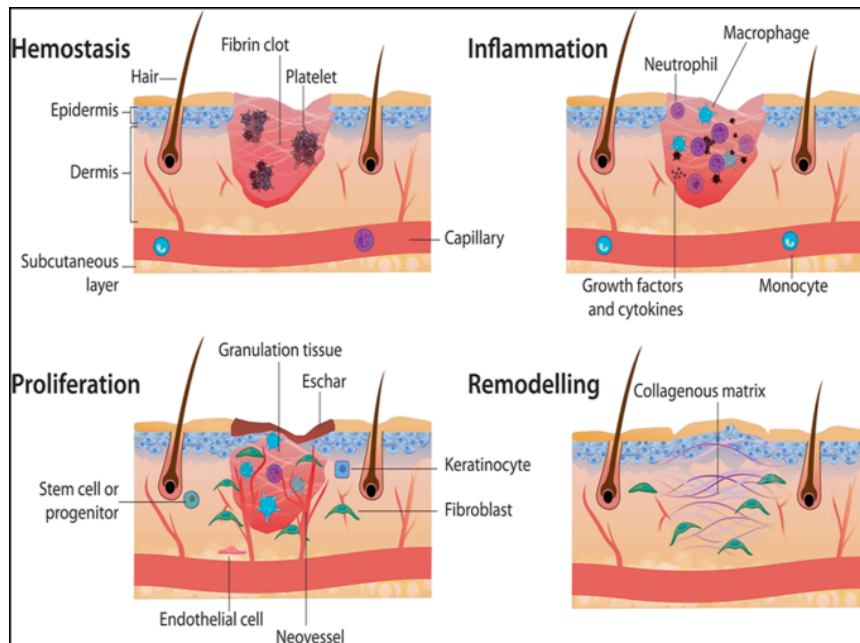
Figure 1. The four stages of wound healing. The process begins with the hemostasis phase, followed by inflammatory phase, proliferative phase, and concluding with the remodeling phase. *Nour et al. 2019. A review of accelerated wound healing approaches: biomaterial- assisted tissue remodeling.*

The fourth phase of wound healing is tissue remodeling, which is the lengthiest phase in the entire process. This phase can take months in order to establish appropriate tensile strength of the skin. Here, the granulation tissue is gradually replaced by functional tissue. Collagen that comprised the granulation tissue is degraded by matrix metalloproteinase enzyme (MMPs) produced by neutrophils, macrophages, and fibroblasts[7]. The ECM evolves into a composition of proteoglycans, glycosaminoglycans, and other proteins, allowing for the further deposition of matrix components[5]. Overtime,

the highly disorganized collagen matrix becomes more crosslinked and aligned along the stress line of the wound in order to improve the tensile strength of the new tissue, and cell and vascular density decrease as scar tissue forms[5,7].

2.2 Chronic Wounds

A wound can be classified as a chronic wound if impaired healing persists for longer than three months[6,11]. Examples of chronic wounds include diabetic foot ulcers, pressure ulcers, and arterial and venous ulcers. Many factors can contribute to the pathogenesis of chronic wounds, such as local factors, regional factors, and systemic factors[1,5]. Although different types of chronic wounds can have differing origins, they are all classified by chronic inflammation of the wound bed, and failure to heal[12]. Chronic wounds often have excessive recruitment of inflammatory cells due to infection, and the increase in the infiltration of leukocytes is triggered by the over-expression of vascular cell adhesion molecule 1 and interstitial cell adhesion molecule 1 from endothelial cells in the wound bed[12].

2.2.1 Reactive Oxygen Species, Hypoxia, and Ischemia in Wound Healing

Notably, excessive accumulation of inflammatory cells leads to the over-production of reactive oxygen species (ROS). High concentrations of ROS can have damaging effects on the ECM, cell membranes, and can lead to cell death[12]. Additionally, instability of the ECM by excessive degradation can cause prolongation of hypoxia in the wound bed, augmenting the chronicity of the wound[12]. Although both ROS and hypoxia occur to some extent in normal wound healing, these factors are exacerbated in chronic wounds playing a role in its failure to heal on its own.

4

In the inflammatory phase of wound healing, immune cells produce ROS to act as a defense mechanism towards bacteria and other foreign material, as well as contribute to chemical signaling including cell motility, cytokine action, and angiogenesis[1,13,14]. In the initial oxidative burst, neutrophils and macrophages release superoxide radicals and hydrogen peroxide. In low concentrations, hydrogen peroxide has shown to act as a chemoattractant, contributing to fibroblast and endothelial cell proliferation, as well as playing a role in angiogenesis[13,14]. However, in the event of excessive oxidative stress, both nonradical (hydrogen peroxide, singlet oxygen) and radical (superoxide anions, hydroxyl radicals) ROS are produced[14]. Due to its high reactivity, excessive ROS can be deleterious to cell migration, proliferation, and survival, as well as damaging to the extracellular matrix[13,14]. Although low levels are common in wound healing, excessive oxidative stress due to high concentrations of free radicals and antioxidants play a major role in the development of chronic wounds.

Hypoxia and ischemia are often associated with chronic wounds due to disturbed vascular supply of oxygen to the wound site. Oxygen tension at the wound site is affected by local blood flow[15]. Therefore, ischemic injuries are often accompanied by hypoxic conditions, although these two phenomena are not the same. In wound healing, oxygen is important because it interacts with cytokines and must be available for consumption by active cells[2]. After injury, hypoxic conditions can result from both limited perfusion of oxygen to the wounds site and increased consumption of oxygen in the inflammatory response[3].

In normal wound healing, oxygen homeostasis is regulated by Hypoxia-inducible factor-1 (HIF-1), a transcription factor that helps cells to adapt to low oxygen tension[3,16].

It is a heterodimer of HIF-1α and HIF-1β. Notably, HIF-1β is detectable in almost all oxygen conditions, while HIF-1α is only detectable during hypoxia[17]. In hypoxia, HIF-1 increases due to the stabilization of HIF-1α via inhibition of its degradation, allowing for dimerization with HIF-1β [16,17]. The activation of this complex results in the transcription of genes related to cell proliferation and angiogenesis[17]. Upon the return to normoxia, HIF-1α is hydroxylated, ubiquitinated, and degraded by prolyl hydroxylase domain-containing protein 2 (PHD2)[17].

Chronic wounds are known to be hypoxic environments. However, despite hypoxia, HIF-1α and HIF-1 levels are reduced in diabetic wounds. The hyperglycemia-induced reduction in these transcription factors is due to the destabilization of HIF-1α, leading to a decrease in the production of genes related to cell proliferation and angiogenesis[3]. In the case of HIF-1α destabilization, it is degraded by PHD2 and cannot dimerize with HIF-1β to form HIF-1. Therefore, the production of wound healing-related genes, such as VEGF, FGF-2, and PDGF, are inhibited, reducing wound healing capabilities.

2.2.2 Other Chronic Wound Pathologies

Another feature of chronic wounds that contributes to the pathology and differentiates them from acute wounds are phenotypic abnormalities in the cells [12,15]. Specifically, fibroblasts and keratinocytes have shown to have phenotypic changes when in the chronic wound environment. Fibroblasts' "chronic wound phenotype", for example, is characterized by a decrease in growth factor receptors and mitogenic potential, resulting in reduced response to cues from the wound environment[12]. In addition, keratinocytes' phenotype in chronic wounds have shown to have an

overexpression of Ki67, reduced migration, and reduced growth factor production[12]. These mechanisms and causes of these phenotypic changes are not fully understood, but better understanding of these molecular pathways has the potential to create new therapeutic targets for chronic wounds.

Biofilms within the wound bed is an additional pathology that can characterize chronic wounds. Chronic wounds are prone to infection, and bacteria that invade the wound bed often form complex polymer matrix structures containing microbes. This matrix acts as a mechanism to circumvent immune defense and develop antibiotic resistance[12]. These biofilms cause a significant delay in the re-epithelialization of the wound, although its mechanism of action is not fully understood.

2.3 Chronic Wound Treatment

Wound care and management is important due to the morbidity associated with chronic wounds[2]. One of the most commonly implemented chronic wound treatments is the removal of non-viable tissue, which can be achieved via autolytic or enzymatic removal. By removing necrotic tissue, the remaining viable tissue allows for cells to proliferate and migrate to the wound and begin the healing process. Following debridement, dressing wounds with protective barriers that help maintain a moist environment is also a common way to treat chronic wounds. Recently, research efforts have expanded into using regenerative engineering strategies to mimic the extracellular matrix to facilitate new tissue growth rather than conventional debridement strategies.

2.3.1 Wound Dressings

Wound dressings are currently the most common treatment for chronic wounds. An ideal wound dressing provides a moist environment, is free of toxic materials, can be

easily removed without further trauma, and has a long shelf life[18]. Wound dressing approaches have been developed to protect the wound, as well as promote wound healing. In 2009, the most commonly used wound dressing in the USA was still wet-to-dry gauze, even with more advanced dressings being clinically available[19]. While they do provide mechanical debridement to the wound, they are not the ideal means for efficient healing that is free of fibrotic tissue. More recently, advanced dressings using both natural and synthetic materials are making their way into clinics to better protect wound areas and promote their healing.

Semi-permeable polymeric films are one category of dressings used to treat chronic wounds. These types of dressings are used because they provide a barrier from microbes and liquid while allowing gas exchange and water vapor permeation[2]. Tegaderm[TM] is an example of a semi-permeable polyurethane film wound dressing currently on the market. However, these types of dressings are commonly used for non-exudative wounds as they are non-absorbent, which would cause accumulation of exudate and subsequent maceration of the underlying wound[2,20,21]. Therefore, the utility of films as wound dressings is limited.

Additionally, hydrogels are commonly used materials to dress wounds[2]. These types of materials are highly hydrophilic, which allows them to absorb wound exudate and keep a moist wound environment. Hydrogels for wound healing have been fabricated from both natural and synthetic polymers. Examples of natural materials that have been investigated for this application include alginate, chitosan, and gelatin. Commonly used synthetic polymers include polyvinyl alcohol, polyvinyl pyrrolidone, and polyethylene

oxide[20]. Often, hydrogels are developed as composites or copolymers of two or more polymers.

Hydrocolloid dressing can often be found as either sheets or hydrocolloid gels, and are commonly composed of carboxymethylcellulose, gelatin, and pectins[21]. They are very hydrophilic materials that are non-adherent and easily removable[20]. They can be used to treat a wide range of wounds, from abrasions to burns to pressure ulcers, and can be worn for longer periods of time, reducing the frequency of dressing changes[20,21]. In granulated wounds with a moderate amount of exudate, hydrocolloids help to maintain the granulation tissue and aid in the re-epithelialization of the wound[21]. They have also shown to keep wound pH low, optimize temperature, and prevent bacterial invasion allowing for cell proliferation and angiogenesis[21]. An example of a clinically available hydrocolloid wound dressing is DuoDerm[TM].

Another class of wound dressings that are commonly used are polymeric foams. Foam wound dressings are commonly used for wounds with a moderate amount of exudate, as long as it does not stick to the wound bed and restrict epithelialization of the wound[21]. Due to the hydrophilicity of some foam dressings, pre-soaking in saline may be necessary as to not dry out the wound. Disadvantages of currently available foam dressings include frequent dressing changes, secondary dressings to limit foam shifting, and less exudate retention compared to hydrogels or hydrocolloid dressings[21].

2.3.2 Regenerative Engineering Approaches

These conventional wound dressings aim to protect wound areas and provide an environment to aid wound healing. More advanced approaches to wound dressings extends on the ideas of traditional wound dressings by integrating ideas from regenerative

engineering principals to help initiate tissue regrowth[22]. These methods combine ideas from mechanical signals, chemical signals, and cells to provide an environment similar to the extracellular matrix that promotes the restoration of normal healing[23]. ECM mimetic materials are being studied to provide a platform for wound support, guidance of tissue growth, and delivery of therapeutics[24]. In addition, the delivery of therapeutics from scaffold, nanoparticles, and other systems are being developed to aid in the regeneration of tissue in a wound. The majority of these technologies are still in developmental stages, yet have growing potential in wound healing applications.

ECM biomimetic materials include hydrogels and scaffolds to facilitate wound healing. The ideal matrix contains a biocompatible material and can be incorporated into the native tissue with little to no rejection. Natural polymers, such as collagen, hyaluronic acid, chitosan, and fibrin are commonly used within a wound-healing scaffold because these components are found in native skin, and therefore promote tissue ingrowth and repair[24]. Acellular matrices are also being studied as potential tissue engineering platforms as they mimic the ECM structurally and mechanically, as well as provide cues that are not found naturally in other scaffold materials. An acellular matrix involves the decellularization of tissues, and studies have shown the utility of decellularized skin, intestinal submucosa, and bladder in dermal burns, diabetic wounds, and urethral repair[23,24]. OASIS Wound Matrix® is a commercially available regenerative wound dressing that is developed via the decellularization of porcine jejunum submucosa layers[24,25]. Alloderm® and Integra® are other examples of tissue engineered skin substitutes. Integra® is a dermal substitute fabricated from bovine collagen, and also possesses a film top layer that is removable once the material has integrated into the

10

wound[26]. Synthetic polymers are also being studied for wound healing scaffold materials, such as polyesters including polycaprolactone (PCL), polylactic acid (PLA), polyglycolide (PGA), and poly(lactic-*co*-glycolide) (PLGA). These are known biocompatible and biodegradable materials that can be tuned to have similar mechanical properties to the skin[24]. Restrata[TM] is a clinically available non-biologic tissue engineered electrospun matrix developed from synthetic polymers to promote wound healing in both acute and chronic wounds. Another example of a biodegradable polyurethane wound dressing is NovoSorb[TM]. NovoSorb[TM] is a foam dressing that hydrolytically degrades while guiding tissue growth into the wound area, and is similar to Integra® in that it possesses a removable over layer seal to avoid spontaneous separation[26].

An additional regenerative engineering strategy that further extends on using materials that facilitate healing is the delivery of therapeutics to chronic wounds by these biocompatible, biodegradable drug carriers. These systems allow for localized delivery, which reduces unwanted side effects and suboptimal delivery that is associated with systemic delivery of drugs[22]. This is especially relevant in chronic wounds due to damaged and reduced vasculature in the wound area[27]. Additionally, modification of the materials allows for modulation of release kinetics of the substance from the carrier, as well as the degradation kinetics of the biodegradable material. As with conventional wound dressings, both natural and synthetic polymers are used to fabricate tissue-regenerative drug delivery systems. Some natural polymers include alginate, fibrin, and chitosan, while some synthetic biomaterials being investigated include PLGA, PCL, and PLLA[22,27]. These materials are used to develop tissue engineering scaffolds, hydrogels, and particles that can deliver a variety of therapeutics to wounds including anti-

inflammatory drugs, growth factors, and gene therapies[22,27]. Regranex® is a clinically available growth factor treatment, which is applied topically to the wound area[28]. However, it has been shown to be ineffective in some chronic wounds, such as venous ulcers, due to improper delivery in a bolus form rather than using a carrier[28,29].

Product	Dressing Type	Material	Uses	Reference
Bioclusive[TM]	Semi-Permeable Film	Polyurethane	Acute Wounds Chronic Wounds	[21,30,31]
Op-Site[TM]	Semi-Permeable Film	Polyurethane	Acute Wounds Chronic Wounds	[18,30,31]
Tegaderm[TM]	Semi-Permeable Film	Polyurethane	Acute Wounds Chronic Wounds	[18,21,30,31]
Allevyn	Tri-Layer Foam	Polyurethane	Highly Exudative Wounds and Burns	[21,30,32]
NovoSorb[TM]	Foam bonded to Film	Polyurethane	Chronic Wounds Burns	[26,33]
Algisite[TM]	Alginate Gel	Calcium-Alginate	Highly Exudative Wounds	[21,30,34]
DuoDerm®	Hydrocolloid	Polyurethane, Polyisobutylene with Gelatin, Pectin, Carboxymethylcellulose	Chronic Wounds Burns	[21,31,35,36]
Integra®	Hydrogel, Tissue Engineered Skin Substitute	Collagen	Acute Wounds Chronic Wounds Burns	[26,30,37,38]
Alloderm®	Tissue Engineered Skin Substitute	Allogeneic Cadaveric Skin Tissue	Acute Wounds Burns	[30,39]
Oasis®	Biological Extracellular Matrix (ECM)	Porcine Small Intestine Submucosa (SIS)	Acute Wounds Chronic Wounds Burns	[25,37]
Restrata[TM]	Non-Biologic Nanofiber Matrix	Polygalactin 910 PLGA, Polydioxanone	Acute Wounds Chronic Wounds	[40,41]

Table 1. Examples of clinically available conventional and tissue-engineered wound dressings for various wound types.

2.4 Antioxidants in Skin and Chronic Wounds

A major pathology seen in chronic wound cases is excessive reactive oxygen species, including peroxide, superoxide, hydroxyl radicals, and singlet oxygen, which can lead to cell death, reduced cell migration and proliferation, as well as damage to the extracellular matrix[13,14]. These effects of excessive ROS impede the normal wound healing process. Antioxidant treatments using biomaterials can act to reduce the various species of ROS common to chronic wounds, and help to restore the wound healing process.

2.4.1 Antioxidants

In general, antioxidants can be described as "any substance that, when present at low concentrations compared to those of an oxidizable substrate, significantly delays or prevents oxidation of that substrate"[42,43]. In this definition, an oxidizable substrates include any substance found in food and living tissues, including lipids, carbohydrates, and proteins[42,43].

The end goal and targets of antioxidants can greatly differ across different scientific fields of study. In the biological and biomedical discipline, antioxidants act as radical scavengers that break down radical chain reactions of existing free radicals or inhibit the production of free radicals in the first place[44]. Free radicals, such as hydroxyl radicals and superoxide, have one or more unpaired electrons, and can lead to DNA mutations, lipid peroxidation of cell membranes, and even cell death[45]. In an oxidative environment, antioxidants will accept or donate electrons to reduce the ROS or free radical, which can either completely eliminate the free radical from the system or transform it into a less severe radical[46]. Antioxidants can also regulate free radical related

enzymes by reducing radical-generating enzymes, such as NAD(P)H oxidase and xanthine oxidase (XO), or inducing the production or activity of enzymes with further antioxidant capacity, such as superoxide dismutase (SOD) and catalase (CAT)[46]. The mechanisms at which antioxidants function can be summarized as follows: 1) blocking free radical chain transfer by scavenging free radicals, 2) inhibiting the production of free radicals, and 3) stimulating the production of additional enzymatic or non-enzymatic antioxidants *in vivo*[47].

There are many methods to evaluate the antioxidant capacity of various substances and materials. The most commonly used assays ate electron transfer based assays, including the Trolox equivalent antioxidant capacity assay (TAC), the FRAP assay, the Cu(II) reduction capacity assay, and the DPPH assay[44]. These methods involve the donation of an electron from the antioxidant to an oxidant probe, causing a color change as a quantifiable measurement of antioxidant capacity. Other less commonly used approaches function on the basis of hydrogen atom transfer (HAT), including the inhibited oxygen uptake (IOU) method, measuring the inhibition of induced lipid autoxidation, and using molecular probes such as the ORAC assay, TRAP assay, and crocin bleaching assay[44]. In these assays, antioxidants and substrate compete for heat-generated peroxyl radicals produced via azo compound decomposition in a complex reaction process.

2.4.2 Intrinsic Antioxidant Capacity of the Skin and Redox Homeostasis

Antioxidants are substances that oppose oxidation or inhibit reactions promoted by oxygen or peroxides[43]. Skin itself has an intrinsic antioxidant system, including both endogenous and exogenous antioxidants that act to reduce ROS and protect tissues[44].

There are both enzymatic and non-enzymatic antioxidants present in this antioxidant system, usually distributed across a gradient in the skin, with higher concentrations commonly found in the stratum corneum of the skin epidermis[48,49]. Enzymatic antioxidants include catalase, glutathione peroxidase (GPx), thioredoxin, superoxide dismutase (SOD), while non-enzymatic examples are ascorbic acid (vitamin C), glutathione (GSH), and sulfhydryls[48]. When there are increases in oxidative stress, the nuclear factor erythroid 2-related factor 2 (Nrf2) signaling pathway is activated to upregulate the transcription of many downstream proteins to increase the intracellular antioxidant capacity in the skin[48,49]. The importance of the particular antioxidant *in vivo* depends on the type of ROS present[49].

In normal healthy tissue, a signaling mechanism known as redox homeostasis regulates the oxidant/antioxidant balance in the tissue. Under normal physiological conditions, there are relatively low levels of ROS due to the balance between its production and removal by skin antioxidants[43]. When the oxidation state is disturbed in the skin either by an increase in ROS or decrease in antioxidant levels, a redox response will be elicited. In the case of chronic wounds, ROS is in such an excess compared to steady state that the intrinsic oxidative stress response is not enough to reduce the intracellular ROS levels and reset redox homeostasis[50]. This failure to maintain redox homeostasis in the tissue leads to adverse affects associated with the pathology of chronic wounds.

2.4.3 Antioxidant Approaches in Tissue Engineering

Recent advances in biomedical research interested in pathologically associated ROS have moved into the development of antioxidant materials for radical scavenging

for applications in tissue engineering. These include biomaterial scaffolds and drug delivery systems that can stimulate regeneration while reducing environmental ROS. Materials that are being explored for tissue engineering applications include natural antioxidants, with some of the most explored including glutathione, ascorbic acid, and polyphenols[47,51]. Synthetic materials with ROS-scavenging bonds within the polymer network are also being explored as potential scaffolds materials for regeneration in oxidative environments[51].

One approach to increasing the antioxidant capacity in tissue engineering systems is through the loading of an antioxidant molecule or drug into a polymeric scaffold. When the scaffold is implanted *in vivo,* the molecule will be released and ROS scavenging will occur. *Lee et al.* developed a 3D printed PCL scaffold with a surface coating of tannic acid (TA) to act as a polyphenol antioxidant followed by immobilization of BMP-2 for bone regeneration. The DPPH assay showed nearly 80% radical inhibition by 24 hours for scaffolds containing TA due to scavenging of the hydroxyl groups on the galloyl residues in TA, as well as maintained cell viability in oxidative environments[52]. In another study, *Marino et al*. doped antioxidant cerium oxide nanoparticles (nanoceria) into electrospun gelatin nanofibers for neuronal regeneration. Nanofibers achieved 1% w/w loading of nanoceria and showed efficient antioxidant capacity in oxidative media and in cell culture[53]. In these approaches, molecules that have antioxidant activity are loaded into the material, but not chemically bonded to the polymers that make up the system.

Another tissue engineering approach implementing antioxidant functionality is through the development of a material that scavenges ROS directly. The benefit in having

a biomaterial with intrinsic antioxidant capacity is there lower risk of losing loaded ROS-scavenging molecules in the preparation process. Rather, the polymer the scaffold is formulated from acts as the antioxidant itself. In a composite scaffold formulated by *Li et al.,* antioxidant glutathione (GSH) was grafted onto carboxyl-capped aniline pentamide (CCAP) via amide linkage with the terminal carboxyl groups, and the resulting pentamer-GSH was used for a composite gelatin/AP-GSH scaffold for cardiac tissue regeneration. *In vitro* scavenging of hydroxyl radicals, superoxide radicals, and DPPH radicals increased with higher GSH percentage, and the high swelling ratio of the scaffolds allowed for greater interaction of grafted GSH with ROS[54]. In a similar approach, *Lith et al.* developed a vascular graft that incorporated ascorbic acid into the polymer network. The resulting poly(1,8-octanediol-co-citrate-co-ascorbate) (POCA) scaffold successfully scavenged free radicals in vitro, as well as inhibited iron chelation and lipid peroxidation[55]. In another system for applications in cardiac tissue regeneration, *Yao et al.* utilized ROS-cleavable thioketal (TK) bonds in a synthetic electrospun fibrous patch to scavenge free radicals in the heart tissue following myocardial infarction. The next section will further discuss TK-based materials for biomedical use in oxidative environments. This fibrous patch showed nearly 80% DPPH radical scavenging by 6 hours by the TK bonds within the patch without the addition of any naturally occurring antioxidants[56].

2.5 Stimuli-Responsive Drug Delivery Systems

Stimuli-responsive materials, also know as "smart materials", are polymers that are designed to change in a controlled manner under the application of internal or external stimuli. These stimuli can be characterized into chemical, physical, and

biological-mediated responsiveness[57]. Stimuli-responsive materials are commonly used for drug delivery applications because they are easily tunable to achieve sustained, controlled release of the cargo, allowing for more effective and efficient delivery of a therapeutic[58].

One of the most common chemical stimulus used in drug delivery is pH, and has been used to deliver drugs from carriers including hydrogels, nanoparticles, and 3-dimesional porous materials[58,59]. Upon changes in environmental pH, bonds can be cleaved, solubility can change, or structural changes can occur within the polymer or polymers. Physical stimuli include light, electricity, and temperature[58]. Thermo-responsive polymers are commonly used, and these materials experience changes in swelling, porosity, and other material properties, allowing for the release of their payload at certain temperatures[58,59]. Enzymes are a common method for biological-mediated release of cargo from a drug carrier. These kinds of materials are optimal in environments that have high levels of enzymes in the tissue or a concentration gradient of enzymes related to the disease[59]. This makes it possible to tailor the material to respond to enzymes associated with a specific disease state. An additional biological stimulus that is gaining attention for drug delivery is reactive oxygen species (ROS), including hydroxyl radicals, superoxide, and peroxide[58]. Altered ROS levels in various disease states have lead to the development of drug carriers that allow for more targeted delivery by using ROS-responsive materials and linkers[60]. In addition to these commonly implemented stimuli in smart biomaterial systems, ultraviolet (UV) irradiation, near-infrared (NIR) light, red light, ultrasound, electricity, and magnetism are being studied as methods to elicit material changes for biomedical applications[60].

Stimulus	Material Change	Examples	Reference
pH	Change in pH causes material swelling	PLGA PEG PDMAEMA	[58]
Temperature	Temperature change results in a change in the polymer-polymer and polymer-water interactions, causing swelling	PNIPAm (PMVE)	[50, 51, 57]
Enzyme	Enzymatic conversion occurs and product causes material swelling	PEG Poly(maleic acid) Poly(vinyl pyrrolidone) Polydimethylsiloxane	[63]
Reactive Oxygen Species	Electron-donating groups cause transfer of charge	Thioether-, selenide/telluride-, oligoproline-, and thioketal-containing polymers	[61]
Light (UV, Red, Near-Infrared)	Light-sensitive chromophore absorbs light increasing the 'local' temperature of the hydrogel, which causes changes in swelling	Spiropyrans (SP) Azobenzenes (Azo) Copper chlorophyllin	[52,55]
Ultrasound	Irradiation causes increase in temperature	Ethylene vinyl alcohol	[58,61]
Electricity	Electric potential causes oxidation/reduction reactions that change polymer charge and/or conformational change	Polyacrylamide	[61]
Magnetism	Magnetic charge causes formation of pores, resulting in changes in swelling	Superparamagnetic iron oxide nanoparticles (SPIONs)	[47, 50]

Table 2. Examples of stimuli used in smart materials for biomedical applications.

2.5.1 pH-Responsive Materials

Drug release triggered by pH is an attractive approach to designing drug delivery systems because the pH levels in the body can vary depending on the target location. For example, the pH of the blood and normal tissues is about 7.4. In contrast, the pH of the gastric fluid is extremely acidic, with a of pH about 1.2, and the pH in an endosome

within a cell is in the range of 5.5-6.0[59]. Tailoring delivery systems to respond to the pH of their environments allows for more targeted delivery to diseases of specific tissues.

Delivery systems that respond to environmental pH can take the form of hydrogels, nanoparticles, 3-dimensional porous structures[65]. Some approaches in designing these materials is to create pH-sensitive linkages between the drug and carrier, or including weakly acidic or basic groups in the polymer backbone that, upon changes in surrounding pH levels, can promote cleavage, solubility, or swelling changes[58]. Cleavage and changes in material solubility or swelling triggers the release of the loaded drug from the system.

Some examples of polymers that have been used in pH-responsive delivery systems include poly(lactic-co-glycolic) acid (PLGA), poly(ethylene glycol) (PEG), poly(acrylamide), and poly(N,N-dimethylaminoethyl methacrylate) (PDMAEMA), among others[58,65]. To tailor the release of the payload based on precise pH levels based upon the target tissue, combinations of pH-sensitive polymers are commonly used to design these systems. Systems that have multiple polymers include ureido-pyrimidinone (UPy) modified PEG hydrogels, N-carboxyethyl chitosan and dibenzaldehyde-terminated poly(ethylene glycol) (PEG) hydrogels, and a block co-polymer of poly(dimethysiloxane) and PDMAEMA[58,59].

2.5.2 Thermo-Responsive Materials

Materials for controlled drug release based on temperature is also largely investigated because of the versatility in design, the tunability of phase transition temperatures, passive targeting capabilities, and *in situ* phase transitions[58,59,65]. They are also relatively easy to formulate and control. The exploitation of the differences in room

temperature and body temperature is used to change the form that the material assumes when introduced to the body.

In response to a certain temperature, thermo-sensitive polymers undergo a volume phase transition, resulting in a change in the solvation state[66]. If a polymer becomes insoluble upon heating, it is said to have a lower critical solution temperature (LCST), and if a polymer becomes soluble upon heating, it has an upper critical solution temperature (UCST)[63]. LCST or UCST systems for drug delivery applications are restricted to aqueous environments because the design of these systems is based on changes in hydration state, which causes volume phase transition[63]. Generally, when these polymers are exposed to their LCST or UCST, their swelling properties change which releases the drug payload.

One of the most commonly studied temperature responsive polymers is poly(N-isopropylacrylamide) (PNIPAM). This is an attractive material for controlled release applications because it is biocompatibility and has an LCST between 25-33°C, independent of the molecular weight or concentration[63]. Another thermo-sensitive polymer interesting for drug delivery applications is poly(methyl vinyl ether) (PMVE), which has a LCST of 37°C[63,66]. These polymers have LCSTs close to physiological temperature, which makes them attractive for controlled drug release applications.

2.5.3 Enzyme-Responsive Materials

Enzymes are useful for controlled release of a therapeutic from a carrier because of their ability to recognize and catalyze physicochemical materials *in vivo*[63]. These systems are especially relevant in diseases in which there is an overexpression or concentration gradient of enzymes specific to the material. Enzyme-mediated release

from a drug carrier allows for the payload to be protected from degradation and clearance during transport and be selectively released once the drug reaches the target tissue, as well as shows enhanced permeability and retention (EPR) when in nanocarriers formulations[58].

These polymers often contain enzyme-reactive labile linkages along the main chain or side groups[58]. Therefore, when catalyzed by an enzyme, these materials can undergo changes in the non-covalent bonds in the structure, leading to self-assembly, morphological changes, or degradation[67]. Another method of utilizing enzymes to mediate the release of a substance from a carrier is by using enzymatic reaction byproducts or intermediates to trigger the release of the payload[67]. A common strategy in the design of enzyme-sensitive polymers is linking enzymatic substrates to amphiphilic copolymers[67]. Often, enzyme-sensitive drug delivery systems are also responsive to other stimuli, including temperature and pH because enzyme-only responsive systems often have a high probability of drug release before reaching its intended target[58]. By using multiple stimuli, the system can more accurately achieve delivery at the intended target and reduce off-target effects.

Enzyme-responsive systems that have been synthesized for biomedical applications are commonly copolymers of two or more polymers. For example, poly(ethylene glycol) (PEG) has been copolymerized to form enzyme cleavable linkages within the copolymer[58]. Other polymers or copolymers that have been used to develop enzyme-responsive drug delivery systems include poly(maleic acid), poly(vinyl pyrrolidone), and polydimethylsiloxane/polyethylenimine[58,67].

2.5.4 ROS-Responsive Materials

Reactive oxygen species (ROS) such as superoxide (O_2^-), hydroxyl radical ($\cdot OH$), hypochlorite ion (OCl^-), and hydrogen peroxide (H_2O_2), are ions that are essential in various physiological functions. However, ROS in excess can be damaging to cells and the ECM, and is relevant in a multitude of diseases and diseased tissues. These large concentrations of damaging ROS has lead researchers to develop drug delivery systems that release their payload when exposed to ROS[58].

ROS-responsive drug delivery systems that have been developed have taken the form of nanoparticles, hydrogels, and 3-dimenstional scaffold structures[60]. The design of polymers and materials that have sensitivity to ROS is achieved by the inclusion of ROS-responsive linkers in polymer complexes[4,57,68–70]. The structures that make up these drug delivery systems often contain thioether, selenide/telluride, oligoproline, and thioketal linkers, among others[60]. Exposure of these linkers to varieties of ROS results in a solubility change, carrier cleavage, or linker cleavage within the complex, allowing for the delivery of the loaded drug[64].

Linkers that undergo solubility changes when exposed to ROS include thioether, selenide, and telluride. Polymers containing thioether linkers undergo phase transition from hydrophobic sulfide to more hydrophilic sulfoxide or sulfone, and monoselenium- or monotellurium-containing polymers also undergo a hydrophobic to hydrophilic phase transition when exposed to ROS[64]. Additionally, oxidation of amino acid residues has shown to cleave the peptide bond in polypeptide linkers such as oligoproline[64]. Thioketal linkers undergo rapid cleavage when exposed to ROS and degraded into acetone and thiol byproducts[64].

2.5.4.1 ROS- Responsive Poly(thio ketal) Materials

23

The scaffolds presented in this work are fabricated from ROS-responsive poly(thio ketal) (PTK) diols for chronic wound healing. When exposed to the high levels of ROS, thioketal materials have shown to be not only degraded by the present hydroxyl radicals, but also scavenge ROS from the enviroment[64]. In a study conducted by Wilson *et al.,* thioketal nanoparticles were selectively degraded by reactive oxygen species, which triggered the release of TNFα siRNA in a murine model of ulcerates colitis[4,56,68,71]. Additionally, Yao *et al.* reports a polyurethane myocardial patch with ROS-degradable thioketal linkages[68].

The poly(thio ketal) urethane (PTK-UR) scaffolds in this work are developed based on methods used by Martin *et al.* Briefly, condensation polymerization is used to synthesize prepolymer from 2-mercaptoethyl ether (MEE) and 1,4-butanedithiol (BDT)[56]. Prepolymer was then hydroxyl-functionalized to allow for crosslinking with isocyanate during foam fabrication[4,68]. The proposed mechanism of degradation upon exposure to ROS is depicted in **Figure 1**[4]. The thioketal linkages within the polymer are destabilized upon exposure to ROS, specifically hydroxyl radicals (OH⁻), resulting in chain scission and breakdown into the initial components, MEE, BDT, and acetone[4].

These relatively small molecules are thought to be rapidly cleared from the body, and previous work shows MEE produces minimal cytotoxicity *in vitro* with mouse fibroblasts, as well as limited *in vivo* host inflammatory response in a mouse model[4]. Throughout the degradation process, the material remains insensitive to hydrolysis, allowing for more controlled degradation characteristics as well as controlled, targeted drug release kinetics.
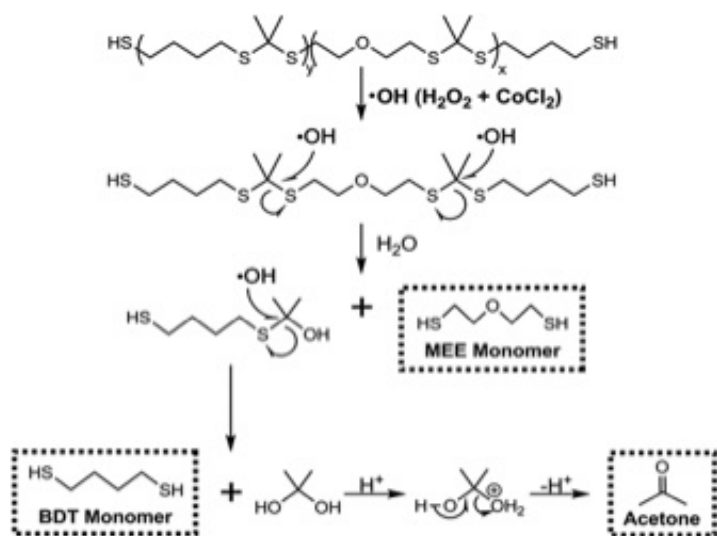
Figure 2. Proposed mechanism of degradation of PTK-UR biomaterials. Scaffolds degrade into initial materials, BDT, MEE, and acetone, which are readily cleared by the body. *Martin, J. R. et al. A porous tissue engineering scaffold selectively degraded by cell-generated reactive oxygen species.*

CHAPTER 3: *In vitro* characterization of hydrophobic/hydrophilic balance and material properties in PTK-UR scaffolds

3.1 Introduction

Biodegradable materials for tissue engineering and regenerative medicine have been broadly studied for the development of scaffolds and other systems. These three-dimensional networks provide a foundation for cell adhesion and tissue growth while also degrading into products that can readily be cleared from the body, allowing for new tissue to take over load-bearing and other functions that the scaffold initially provided[72,73]. Due to certain disadvantages of natural polymers, such as complex structural networks and immunogenicity, synthetic polymers have become more extensively investigated for a variety of tissue engineering applications due to the tunability of networks, high processing flexibility, and low risk of immunogenicity[74,75]. Examples of synthetic polymers that have gained greatest attention by researchers include poly-(ε-caprolactone) (PCL)[76,77], poly-lactic-glycolic acid (PLGA)[78,79], and polyurethanes[80,81].

Polyester urethanes (PEURs) are one class of polymer that has gained recent attention to form three-dimensional porous structures for tissue engineering and regenerative medicine. Foams formulated from polyester urethanes also contains components including polyol, isocyanate as a crosslinking agent, reaction catalyst, and water as a blowing agent to induce pore creation in the foam[81]. Aliphatic ester linkages in PEURs render them susceptible to hydrolytic degradation, in which they degrade into initial components and can be cleared from the body[82]. Polyol and isocyanate structures

can also be modified in order to tune degradation properties and stimuli in PEUR biomaterials[83,84].

Notably, the modification of polyol structure or addition of certain types of bonds in polyester urethanes can create systems whose properties change in response to their environment. This includes self-healing, shape memory, and shear-thinning polyester urethanes[85–87]. Scaffolds explored here are formulated with polyols that contain thioketal bonds, which are selectively degraded by reactive oxygen species, specifically hydroxyl radicals[68]. The thioketal linkages within the polymer are destabilized upon exposure to ROS, resulting in chain scission and breakdown of the material[4]. The ROS-responsive nature of these materials make them attractive for wound healing applications due to the high levels of ROS in the chronic wound environment.

3.2 Materials and Methods

Materials

Tertiary amine catalyst (TEGOAMIN33) was obtained from Goldschmidt (Hopewell, VA) and Lysine Triisocyanate (LTI) was acquired from Kyowa Hakko USA (Tokyo, JP). Cobalt chloride and hydrogen peroxide were purchased Fisher Scientific (Pittsburg, PA).

Polymer Synthesis

Polymers were synthesized based on previously established methods[88]. PTK diols were synthesized via condensation polymerization in acetonitrile at 80°C using MEE, 2,2-dimethoxypropanone (DMP), and p-toluenesulfonic acid catalyst. Briefly, p-toluenesulfonic acid monohydrate (PTSA) was added to a tri-necked boiling flask with an attached addition funnel. These were placed under vacuum 15 minutes prior to being

purged with nitrogen. The boiling flask was charged with anhydrous acetonitrile and MEE and BDT in amounts specific to the batch being made. The additional funnel was charged with anhydrous acetonitrile and 2,2-dimethoxypropane (DMP). To ensure polymers with free terminal thiols, a molar excess of dithiol monomers relative to DMP was used. The addition funnel and boiling flask were purged with nitrogen for 30 minutes, and then the boiling flask was submerged into an oil bath at 80°C for temperature equilibration. After 15 minutes, the funnel stopcock was set, followed by the dropwise addition of acetonitrile-DMP into the boiling flask for 16 hours, continuously stirring. Acetonitrile was removed my rotary evaporation and the PTK diols were isolated via precipitation in cold ethanol, and then dried under vacuum. The isolated PTKs were then reacted with 2-bromoethanol and cesium carbonate for hydroxyl functionalization to allow for the diols to be reacted with isocyanates.

Scaffold Synthesis

The poly(thio ketal) urethane and polyester urethane scaffolds were prepared using two-component reactive liquid molding of Lysine Triisocyanate (LTI) and a hardener component comprising of the PTK diol, deionized water, TEGOAMIN33 catalyst, Turkey Red oil stabilizer, and calcium stearate pore opener. First, the calcium stearate, Turkey red oil, DI water, and PTK diol were added to the mold and mixed for 30 s at 3300 rpm in a Hauschild DAC 150 FVZ-K SpeedMixer (FlackTek, Inc., Landrum, SC). Next, the LTI was added dropwise and the mixture was mixed for an additional minute. This mixture was then allowed to rise for 10-20 minutes at 37°C for complete setting. Scaffolds were allowed to set for 24 hours before being removed from molds.

Table A1 shows parts per hundred parts polyol (PPHP) used to formulate scaffolds for each polyol.

Polymer Film Synthesis

PTK-UR films used for contact angle measurement were made using FisherBrand (Pittsburg, PA) polyethylene molds with a diameter of 22 mm. Briefly, the PTK diol and bismuth catalyst were mixed for 30s at 3300 rpm in a Hauschild DAC 150 FVZ-K SpeedMixer (FlackTek, Inc., Landrum, SC). The polyol/bismuth was mixed an additional 30s if mixture was not spread across entire bottom of mold. Next, Lysine Triisocyanate (LTI) was quickly added to the diol/bismuth mixture. The film components were mixed for an additional minute in the SpeedMixer. Films were allowed to cure for 24 hours before removal from the molds. Table A2 shows parts per hundred parts polyol (PPHP) used to formulate films for each polyol.

Differential Scanning Calorimetry

For Differential scanning calorimetry (DSC) and glass transition temperature (T_g) analysis, samples ranging in mass from 5 to 9 mg were heated from -80.0^oC to 20.0^oC at a rate of 10^oC min^{-1} on a TA (New Castle, DE) Q200 DSC. Samples were then cooled to -80.0^oC at a rate of 10^oC min^{-1}, and heated a second time to 30^oC at a rate of 10^oC min^{-}1. All transitions were obtained from the second heating run.

Soluble Fraction

Freshly made scaffolds were allowed to cure overnight prior to measurements. Initial dry mass was taken, and scaffold pieces were incubated in dichloromethane for 24 hours. DCM was removed and the scaffolds were allowed to air dry for 24 hours prior to

final mass measurement. Soluble fraction for each scaffold formulation was calculated via equation. 1.

$$f_s = 100 - \left[\frac{M_0 - M_f}{M_0} * 100\right]$$

Equation 1. Soluble fraction determination of PTK-UR scaffolds.

In this equation, f_s is the soluble fraction, M_0 is the initial scaffold mass, and M_f is the final mass after drying.

Core Density and Core Porosity

Scaffolds of 1000mm^3 were formulated, and dry mass, height, depth, and width were measured. The volume was calculated and these values were used in equation 2 to find core density, ρ_c.

$$\rho_c = \frac{M}{V} * 10^6$$

Equation 2. Core density of PTK-UR scaffolds.

Core porosity was calculated via equation 3 using the core density previously found using equation 2.

$$\varepsilon_c = 1 - \left(\frac{\rho_c}{\rho_P}\right)\frac{\rho_P - \rho_A\rho_P/\rho_C}{\rho_P - \rho_A}$$

Equation 3. Core porosity of PTK-UR scaffolds using core density from Equation 2.

Here, ε_c is core porosity, and ρ_A, ρ_c, and ρ_p are density of air, core density, polymer density, and, respectively.

Crosslink Density

Scaffold (n=3) initial dry mass was measured and subsequently incubated in DCM for 24 hours. Following swelling, scaffolds were gently dabbed prior to final swollen mass measurement. Crosslink density was calculated via equations 4-6 using dry mass, ω_0, swollen mass, ω_s, and polymer and solvent density, d_p and d_s, respectively.

$$V_{equil} = \frac{\omega_0}{d_p} + \frac{\omega_s - \omega_0}{d_s}$$

Equation 4. Equilibrium volume of swollen PTK-UR scaffolds.

$$V_r = \frac{\omega_0}{V_{equil} X d_p}$$

Equation 5. Equilibrium volume fraction of swollen scaffold for polymer of interest.

$$M_c = \frac{\bar{V}_s d_p \left(V_r^{\frac{1}{3}} - \frac{V_r}{2} \right)}{-[\ln(1 - V_r) + V_r + X V_r^2]}$$

Equation 6. Flory-Rhener equation for molecular weight between crosslinks of PTK-UR scaffolds.

$$v_c = \frac{1}{M_c}$$

Equation 7. Crosslink density of PTK-UR scaffolds.

Equations 4 and 5 are used to calculate parameters to be used for the determination of molecular weight between crosslinks, M_c. V_{equil} is the equilibrium volume of the swollen network, and V_r is the equilibrium volume fraction of the polymer of interest in the foam. Parameter X is the solvent-polymer interaction parameter, which is assumed to be 0.5. $\bar{V}_s$ is the molar volume of the solvent, DCM.

Contact Angle

Contact angle for each polyol was done using a Rame-Hart (Mountain Lakes, NJ) Model A-100 contact angle goniometer. A droplet of water was dispensed from the needle onto the surface of a polymer film formed using the polyol and lysine triisocyanate with bismuth neodecanoate catalyst, as described previously. The degree of droplet spreading was achieved by measuring the resulting contact angle of the water droplet with the surface of the film. Contact angle for both the left and right sides of the droplet was measured. Measurements were taken using three experimental replicates for

three different batches of polymer films, and three technical replicates were used for each batch.

Swell Ratio

Swell ratio was used as a measurement of hydrophilicity. The dry mass of scaffold pieces was taken, and scaffolds were then soaked in PBS overnight. The swollen mass was taken after 24 hours of incubation. The swell ratio was calculated by the equation represented in Eq. 1.

$$\% \, Swelling = \frac{M_s - M_d}{M_d} * 100$$

Equation 8. Swell ratio of PTK-UR scaffolds.

In this equation, M_s is the swollen wet mass, and M_d is dry mass of the scaffold pieces. Swell ratio for scaffolds was also measured over the degradation period to further analyze the hydrophilic/hydrophobic balance of the material during incubation in PBS and 2% H_2O_2 with 0.01M $CoCl_2$.

Dynamic Mechanical Analysis

Young's Modulus was measured in compression at 37°C in a compression clamp using the TA (New Castle, DE) Q800 Dynamic Mechanical Analyzer. Cylindrical scaffold punches 6mm in height and 6mm in diameter were used to perform both wet and dry mechanical analyses. A preload force of 0.1N was used, and scaffolds were compressed along the longitudinal axis at 10% strain min^{-1} until 60% strain was reached. The longitudinal compression was repeated in three separate runs for each scaffold punch. Scaffold punches for wet measurements were incubated in PBS for 24 hours prior to testing and were allowed to recover in PBS for 45 minutes in between runs. The Young's modulus was calculated by taking the slope of the linear region of the stress-

strain curve after initial toe-in for each respective scaffold. Three experimental replicate

scaffolds were tested using three different batches of polymer, and two technical

replicates were tested for each batch.

ROS-Mediated Scaffold Degradation

Scaffold pieces of 10mg were exposed to PBS, 0.2% H_2O_2/0.001M $CoCl_2$, 2%

H_2O_2/0.01M $CoCl_2$, or 20% H_2O_2/0.1M $CoCl_2$ for up to 20 days. Degradation media was

replaced every other day. At each time point, degradation media was removed and

scaffold pieces were washed 3 times with PBS. Degradation media was reserved for

analysis. Scaffolds were lyophilized overnight and final mass was taken. Degradation

was taken as percent mass loss for each time point using Eq. 2.

$$\% \ Mass \ Remaining = \frac{M_t}{M_0} * 100$$

Equation 9. Determination of PTK-UR scaffold mass loss in oxidative media.

In this equation, M_t is the mass of the scaffold at time t, and M_0 is the initial scaffold

mass following initial ethanol wash.

Mathematical Modeling of PTK-UR ROS-Mediated Degradation

MATLAB (Mathworks, Natick, MA) was used to fit the oxidative degradation

kinetics of PTK-UR scaffolds to a first order mathematical model based on H_2O_2

concentration using Eq. 3.

$$\frac{M_t}{M_0} = e^{-kt}$$

Equation 10. First order model of degradation kinetics.

In this equation, M_t is the scaffold mass remaining at time t, M_0 is the initial scaffold

mass, and k is the degradation rate constant. Non-linear regression was used to fit the

scaffold degradation data to the first order mathematical model and to determine the

degradation rate constant for each scaffold with respect to the degradation media concentration.

Scanning Electron Microscopy

Scaffold pieces of 60-80mg were exposed to PBS or 2% H_2O_2 with 0.01M $CoCl_2$ for up to 15 days. Degradation media was replaced every other day. At each time point, degraded scaffolds were washed with an ethanol series 2 times for 10 minutes in each concentration in the following series: 30%, 50%, 70%, 80%, 90%, 95%, 100%. Following the ethanol series, scaffolds were dried via critical point drying using the EMS 850 Critical Point Dryer with ethanol as the exchange fluid. Pore structure of degraded scaffolds was imaged using a Zeiss (Jena, DEU) Merlin Scanning Electron Microscope with Gemini II column. After the final mass was taken, scaffold pieces were mounted onto an SEM stub using carbon tape. Scaffolds were sputter coated in gold using a Cressington Sputter Coater prior to imaging. Images were taken using the Everhart-Thornley secondary electron detector at a beam voltage of 3.00 keV or 10.00 keV.

Statistics

All reported data are presented as the mean and standard deviation of the mean. Statistical analysis was performed using single factor analysis of variance (ANOVA) and Tukey's multiple comparison tests, with p-values less than 0.05 being considered as statistically significant.

3.3 Results

Physical Characteristics of PTK Polyols and Formation of Scaffolds
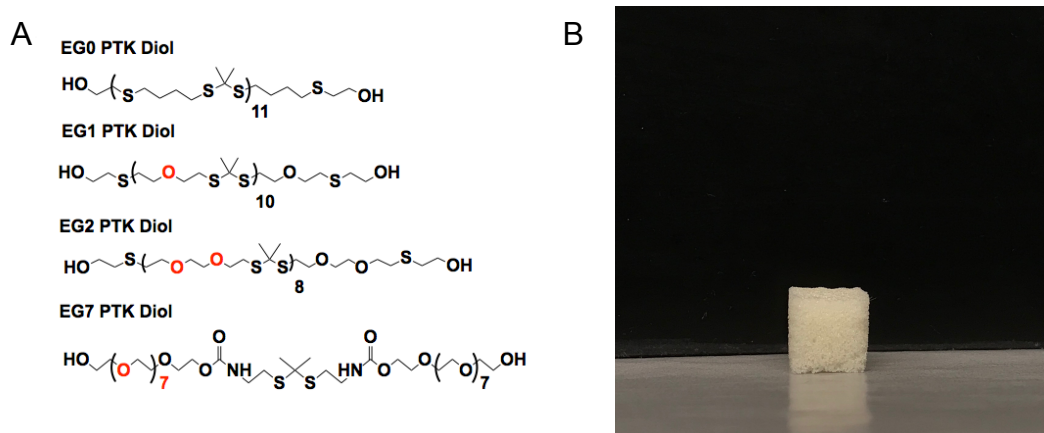
Figure 3. Poly(thio ketal) polymers and scaffolds. (A) PTK monomer structures, (B) PTK-UR foam scaffold formulated from EG7 PTK diol

Differential Scanning Calorimetry was done to determine the glass transition temperatures of PTK-UR diols. Glass transitions for EG0, EG1, EG2, and EG7 were measured as -56.29, -59.57, -62.09, and -48.02, respectively.

	Sol Fraction (%)	Core Porosity (%)	M_c (kg/mol)	v_c (10^{-6})
900t	1.6% ± 0.9%	87.6% ± 1.3%	201.65	5.095
1500t	3.3% ± 3.1%	86.6% ± 2.4%	165.77	6.15
EG0	4.5% ± 1.2%	85.9% ± 5.6%	282.18	3.56
EG1	1.6% ± 0.7%	85.6% ± 1.7%	145.65	7.47
EG2	4.6% ± 2.0%	87.0% ± 1.8%	192.86	5.19
EG7	5.4% ± 7.0%	90.8% ± 0.04%	563.68	1.81

Table 3. Physical properties of PTK-UR and PEUR scaffolds.

Soluble Fraction was used to analyze the amount of soluble, unreacted components present in scaffolds following foaming and curing overnight. PEUR controls (900t, 1500t) and PTK-UR scaffolds possessed similar sol fractions following incubation in DCM for 24 hours (**Table 3**). Core Porosity for scaffolds 1000 mm^3 in volume was

measured, with comparable porosities measured for both PEUR scaffolds and PTK-UR scaffolds (**Table 3**).

The molecular weight between crosslinks and crosslink density can be found in **Table 3**. Comparable M_c and v_c measurements were found for the PEUR scaffolds and EG0, EG1, and EG2, but EG7 had significantly larger molecular weight between crosslinks and lower crosslink density. As PEG content in the EG1, EG2, and EG7 monomers increased, the M_c increased and v_c decreased.

Hydrophilicity Analysis of PTK-UR Scaffolds

Contact angle of polymer films and swell ratio of the library of PTK-UR scaffolds was performed to determined hydrophilicity changes with increased polyethylene glycol content in polyols. As the PEG content increased, the angle of water droplets dispensed on the surface of films decreased. Angles of EG0, EG1, EG2, and EG7 were measured as 79°, 66°, 61°, and 52°, respectively (**Figure 4**). More hydrophobic 900t and 1500t PEUR film contact angles were 75.2^{o} and 75.4^{o}, respectively. Additionally, as PEG content increased, the degree of foam swelling increased due to higher hydrophilicity shown in **Figure 4**.
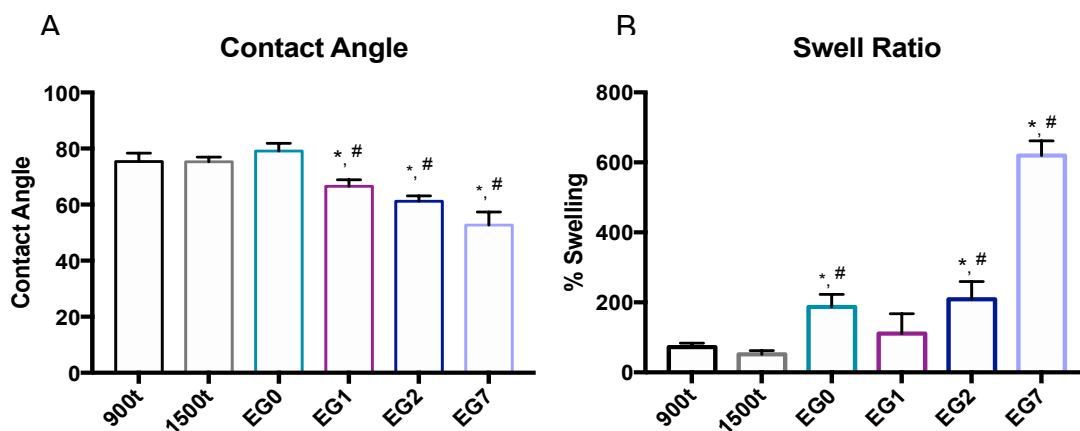

Figure 4. Hydrophilicity of PTK-UR polymers. (A) Contact angle measurements on thin polymer films. (B) Swell ratio of scaffolds incubated in PBS. *$p < 0.05$ compared to 900t-PEUR. #$p < 0.05$ compared to 1500t-PEUR.

Mechanical Analysis of PTK-UR Scaffolds

Dynamic mechanical analysis (DMA) was done to determine the Young's Modulus of dry and wet scaffolds. Cylindrical 6mm x 6mm scaffolds were tested under compression at 10% strain min^{-1} until 60% strain was reached. For wet measurements, scaffolds of the same size were incubated in PBS for 24 hours prior to testing. Moduli for each formulation are shown in **Figure 5**. There are no significant differences in moduli across the library of scaffolds as PEG content increases. Additionally, scaffold moduli remain in the same range as conventional PEUR scaffolds, including the 900t PEUR and 1500t PEUR used in these studies.
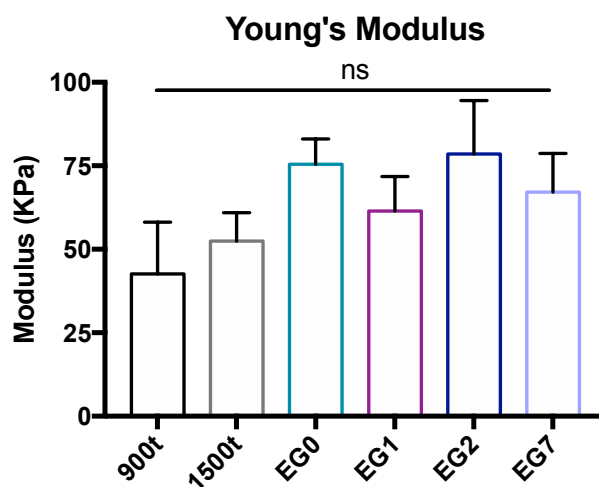
Figure 5. Mechanical properties of PTK-UR and PEUR scaffolds. The compressive moduli were taken under aqueous conditions at 37ºC. There are no significant differences in measured moduli for any of the scaffolds.

Degradation Kinetics of PTK-UR Scaffolds

Scaffold pieces were incubated in phosphate buffered saline or oxidative media containing 20%, 2%, or 0.2% hydrogen peroxide and cobalt chloride for up to 20 days. At each respective time point, scaffolds were dried. Final mass was measured and data is presented as percent mass remaining. PTK-UR scaffolds show a dose-dependent degradation dependent in media hydroxyl concentration, but remain stable in media

absent of ROS as shown in **Figure 6, A-D**. EG7 degrades the most rapidly in all

oxidative media conditions, and EG1, EG2, and EG7 scaffolds are completely degraded

by day 7 in 20% H_2O_2. PEUR scaffolds 900t and 1500t are stable in both oxidative media

and PBS. Representative SEM images in **Figure 7** and **Figure 8** show degradation of

PTK-UR scaffolds from those exposed to 2% H_2O_2 media, and show surface pitting and

collapse of pore structure over 15 days, while these morphological changes were not

evident in scaffolds incubated in PBS or PEUR scaffolds incubated in both oxidative

media and PBS.
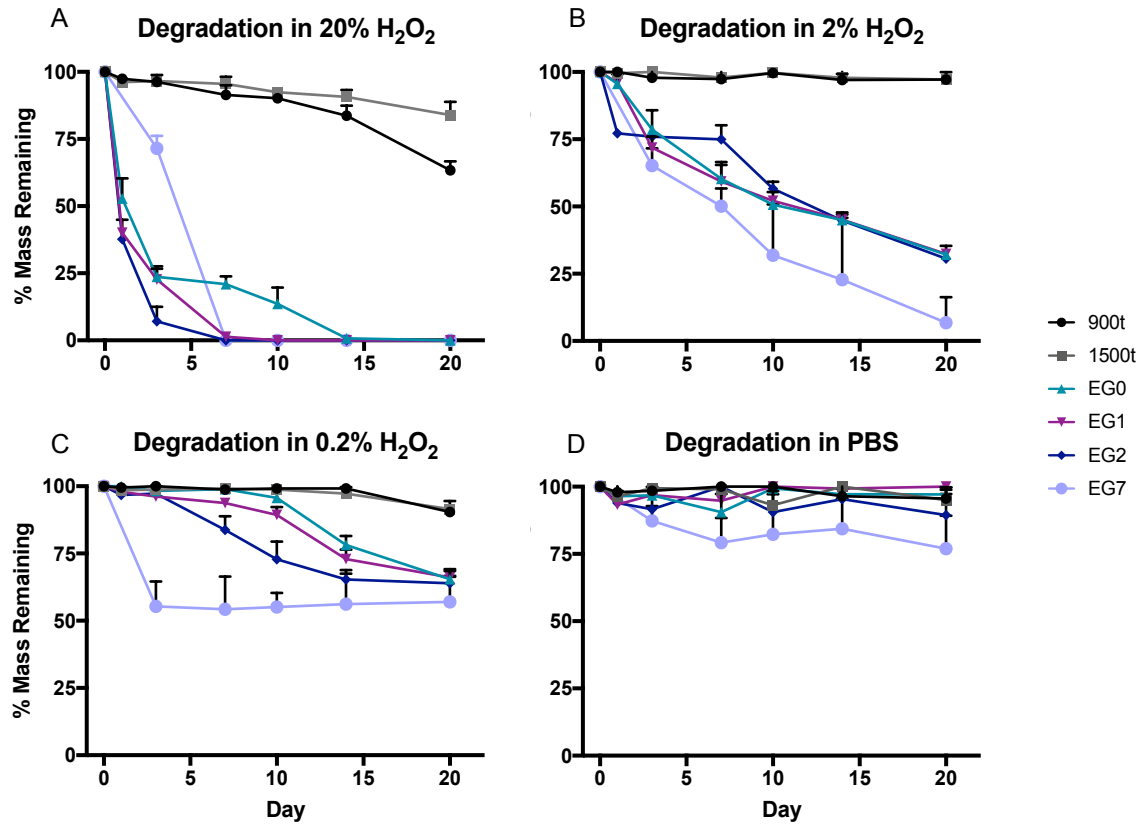
Figure 6. Degradation kinetics of PTK-UR and PEUR scaffolds in oxidative media. Scaffolds degradation is directly related media concentration. Data presented as percent scaffold mass remaining in (A) 20% H_2O_2/0.1 $CoCl_2$, (B) 2% H_2O_2/0.1 $CoCl_2$, (C) 0.2% H_2O_2/0.1 $CoCl_2$, (D) PBS.
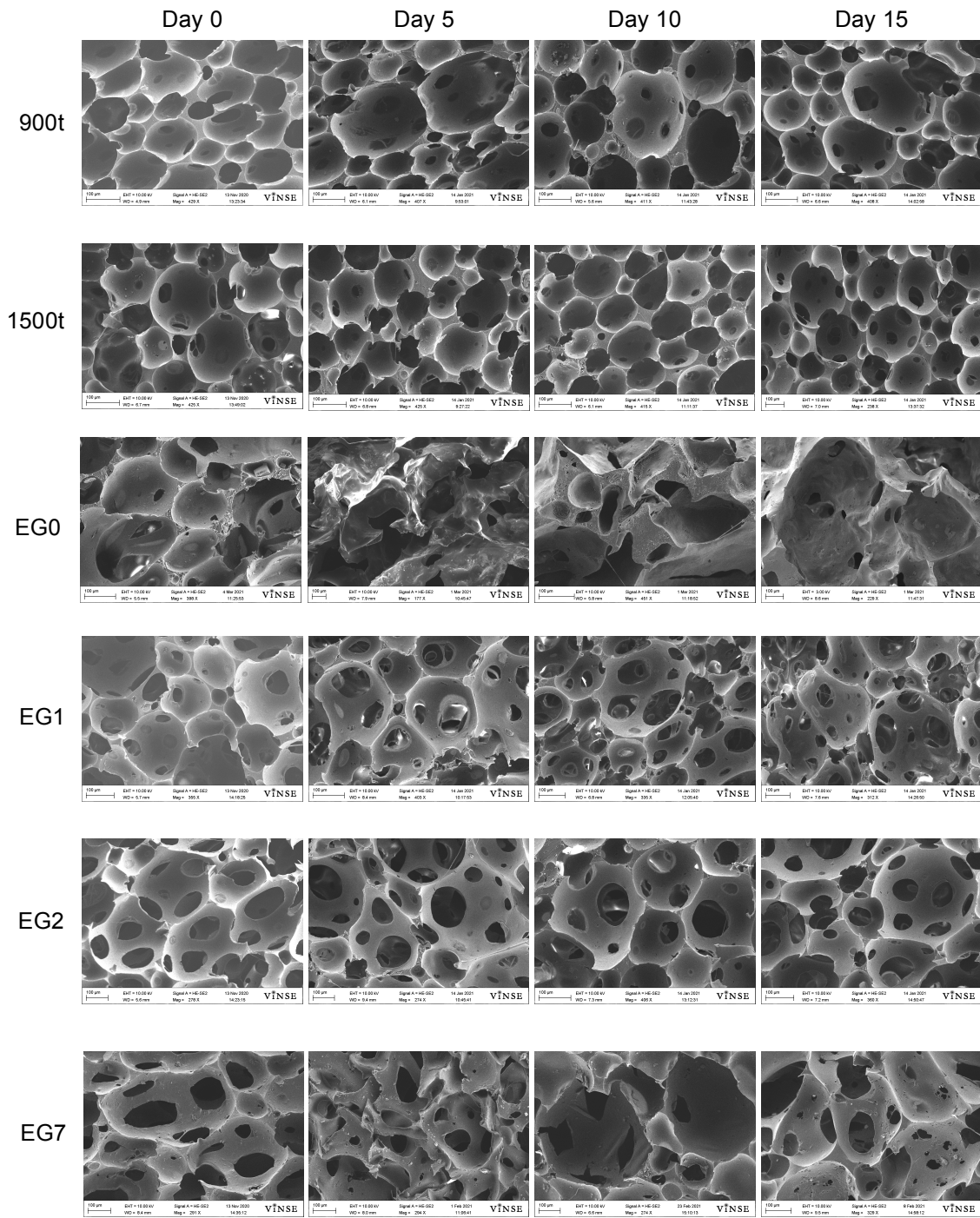
Figure 7. Representative SEM images of scaffold pore structure after being incubated in PBS for up to 15 days. Scaffolds were dried via critical point drying and sputter coated in gold prior to imaging
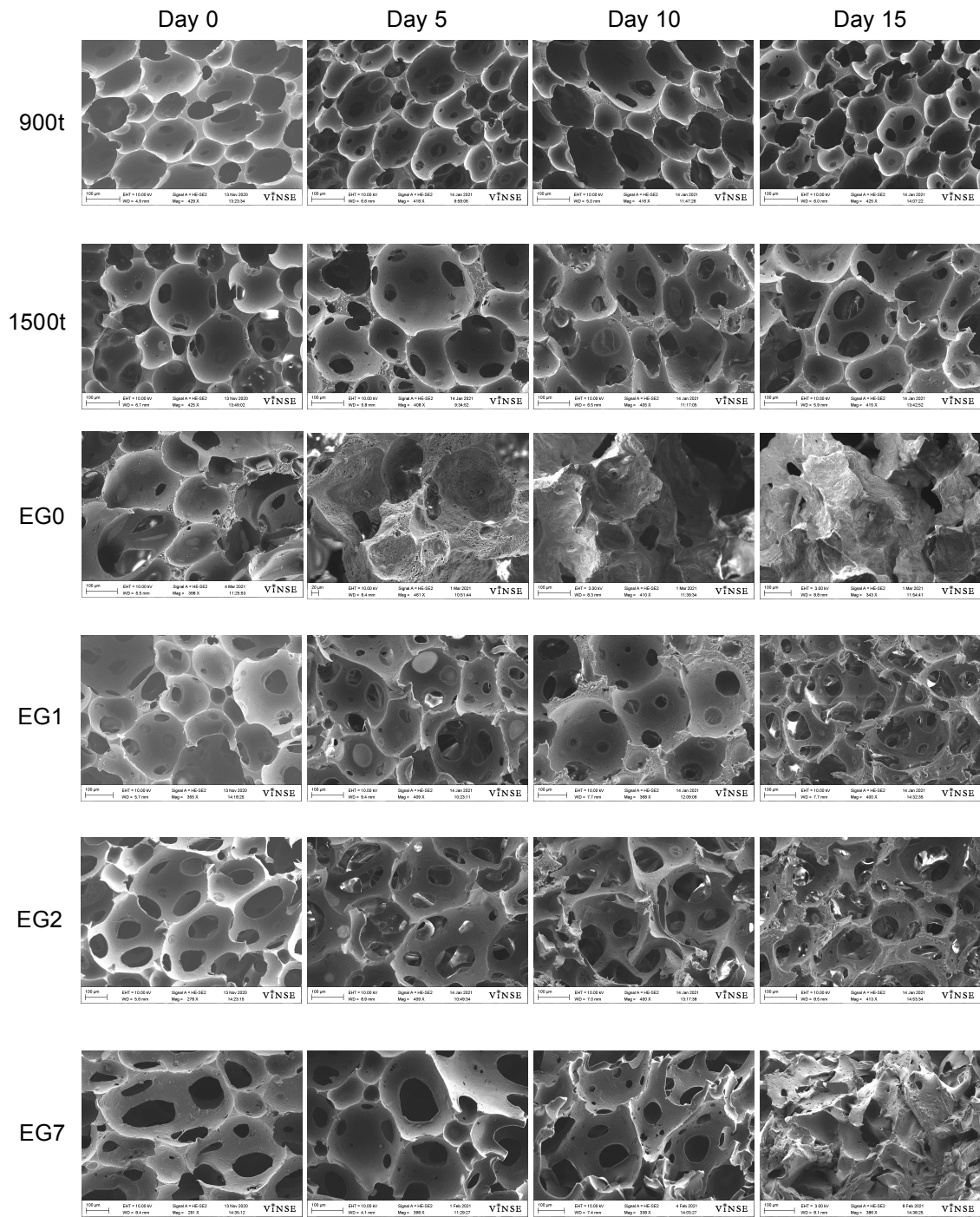
Figure 8. Representative SEM images of scaffolds incubated in 2% H_2O_2/0.01M $CoCl_2$ for up to 15 days. Scaffolds were dried via critical point drying and sputter coated in gold prior to imaging.

To further investigate the effect of ROS on PTK-UR scaffolds, MATLAB was used to fit the mass loss kinetics to a first order mathematical model with respect to hydrogen peroxide concentration (Equation 10). The degradation profiles from MATLAB in **Figure A1** display both model-generated curves as dotted lines and experimental data as solid lines. The derived degradation rates for scaffolds in respective media conditions are shown in **Figure 9**, where the degradation rate constant of EG7 scaffolds is significantly greater than PEURs (900t and 1500t) for both 2% H_2O_2/0.01M $CoCl_2$ and 0.2% H_2O_2/0.001M $CoCl_2$. The other PTK-UR formulations (EG0, EG1, and EG2) have significantly higher degradation rates than PEURs for 2% H_2O_2/0.01M $CoCl_2$.

Degradation Rate Constants
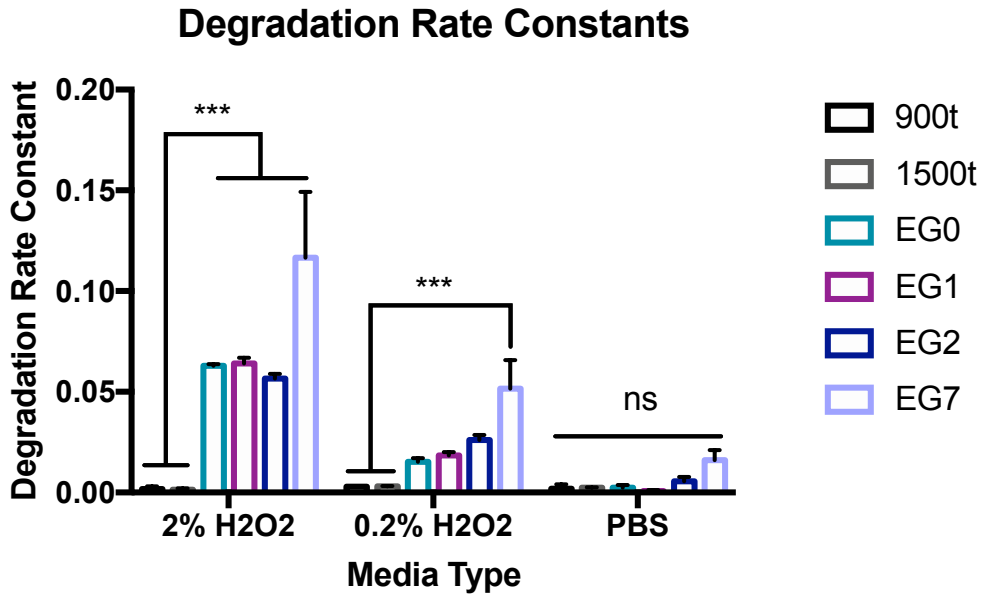
Figure 9. Degradation rate constants for PTK-UR and PEUR scaffolds in oxidative media and PBS used to generate best-fit curves. Values are calculated from MATLAB first-order degradation model, *p < 0.05.

3.4 Discussion

Conventional scaffolds commonly used for tissue engineering applications feature bonds that are hydrolytically degradable. Cleavage of ester bonds by hydrolysis causes autocatalytic degradation driven by carboxylic acid groups, leading to acidification of the

environment that further delays the healing process[89]. In polyester urethanes specifically, scission of ester bonds breaks the main chain into smaller chains, one end with a hydroxyl and the other end with an acidic carboxyl group. The carboxylic acid group further accelerates hydrolysis of polyester chains and turns autocatalytic[90,91]. Presented here are 4 variants of poly(thio ketal) urethane scaffolds for wound healing that undergo cell-mediated oxidative degradation by environmental ROS, while remaining resistant to hydrolysis[68]. It has been shown that fine-tuning degradation rates to match tissue regeneration rates are important for optimal healing[89,92]. Tuning properties of PTK polymers by avoiding hydrolytic and subsequent autocatalytic degradation is expected to promote better matching of degradation rate to cellular remodeling and regeneration.

PTK-UR polymers synthesized here possess similar M_n values of about 2000 Da. Thermal analysis of the diols yields T_g values that are similar to those reported for PTK-UR diols by *Martin et al*[4]. Scaffolds were formed by reaction of lysine triisocyanate with 4 variants of PTK diols, EG0, EG1, EG2, and EG7, with each monomer containing increasing units of polyethylene glycol, respectively. To analyze reaction efficiency, sol fraction was measured by taking initial mass, incubating scaffolds in dichloromethane for 24 hours, and taking final mass after drying. The relatively low sol fraction values indicate the isocyanate and diols were well matched and effectively reacted during scaffold formulation. PTK-UR scaffolds were 85-90% porous, which is similar to porosity found for PEUR scaffold controls. This degree of porosity is an important feature for tissue engineering scaffolds to promote optimal cellular in-growth, nutrient and waste exchange, and the development of vascular networks[4].

Polyester urethane materials, such as the 900t and 1500t used here, are hydrophobic. In wound healing applications, foam dressings are designed to have sufficient exudate absorbency while maintaining a moist environment needed for tissue repair[93]. In the presented PTK-UR scaffolds, increased PEG content in the polyols was used to increase the hydrophilicity of the foams. As expected, evident by the contact angle of polymer films and swell ratio of the foams, increasing PEG in the polyol formulations effectively changes the hydrophilic profile of the materials. The PEURs (900t and 1500t) and EG0, whose monomers contain no PEG, were the most hydrophobic, with contact angles of 79°, 75.2° and 75.4° and swell ratios of 72.5%, 51.7%, and 186.9%, respectively. When PEG was present to the diols, such as in EG1, EG2, and EG7, contact angles were measured as 66°, 61°, and 52°, and swell ratios were measured as 111%, 218.7%, and 619.7 respectively. Interestingly, changes in hydrophilicity of the scaffolds do not significantly change the mechanical properties, specifically the Young's modulus. There is no trend in the modulus between scaffolds, therefore, it can be hypothesized that water uptake is more important than mechanical properties for integration into the wound *in vivo*. As PEG content in the PTK-UR scaffolds increased, molecular weight between crosslinks increased and crosslink density decreased. Research on other castor-oil based polyurethanes that contain PEG have also shown an increase in Mc as PEG chain length increases, as well as an inverse relationship between PEG content and glass transition temperature[94]. There is no observed relationship between the crosslink density and the elastic modulus of the scaffolds.

Previous works have investigated cell-driven degradation mediated by reactive oxygen species[4,68,71]. PTK-UR scaffolds here were formulated with lysine triisocyanate

(LTI) due to increased tissue infiltration in an ischemic wound model compared to hexamethylene diisocyanate trimer (HDIt)[71]. Oxidative degradation was tested by exposing scaffolds to oxidative media at 20%, 2%, and 0.2% H_2O_2 with 0.1, 0.01, and 0.001M $CoCl_2$, respectively. Media containing H_2O_2 and $CoCl_2$ undergoes an Electro-Fenton-like reaction to produce hydroxyl radicals[95]. These radicals destabilize thioketal linkages and cause chain scission and breakdown of the material. As the PEG content, and subsequently the hydrophilicity, of the scaffold increased, the degradation rate in oxidative media increased. When fitted to a MATLAB first order degradation model, rate constants for media containing H_2O_2 increased with PEG content for EG0, EG1, EG2, and EG7. PEUR controls (900t and 1500t) are less responsive to ROS and have lower rate constants. When scaffolds are exposed to aqueous oxidative environments, high degrees of swelling allow for more exposure of TK linkages within the matrix. Greater exposure increases accessibility for ROS to destabilize these bonds, resulting in accelerated degradation kinetics. Representative SEM images of EG-series scaffolds exposed to 2% H_2O_2/0.01M $CoCl_2$ show evident of degradation over 15 days, with loss of pore structure and surface pitting occurring as soon as 5 days. By day 15, EG7 scaffolds show complete loss of structure, while EG1 and EG2 also exhibit increased surface pitting and widening of pores. Interestingly, PEG-containing scaffolds exhibited some mass loss in phosphate buffered saline free of ROS. These degradation characteristics can be attributed to LTI being more susceptible to hydrolytic degradation compared to HDIt, which has shown to be more stable in aqueous conditions[71]. Although there is slight mass loss for scaffolds incubated in PBS, representative SEM images show that scaffolds maintain pore structure and integrity up to 15 days, with only slight collapse being

observed for EG7 scaffolds. Due to excessive swelling of EG7 foams, scaffold structure following drying is affected likely do to mechanical disruption by the high degree of water absorption.

3.5 Conclusion

The balance of hydrophobic and hydrophilic properties in biomaterials is key factor in the design of wound healing dressings in order to absorb wound exudate and maintain a moist environment. Additionally, in the wound environment, reactive oxygen species is a key mediator of inflammatory responses in cells and tissues. Presented here is a series of poly(thio ketal) polymers that feature ROS-responsive bonds and contain varying amounts of polyethylene glycol to modulate their hydrophilicities. These polymers were successfully incorporated into 3D porous PTK-urethane scaffolds that showed similar mechanical properties similar to conventional polyester urethane scaffolds that have been used for tissue engineering applications. PTK-UR scaffolds formulated with lysine triisocyanate were selectively degraded by ROS while remaining relatively stable in aqueous conditions. Accordingly, oxidative degradation rates *in vitro* followed first order degradation kinetics with respect to ROS concentration and scaffolds hydrophilicity. All in all, these data provide evidence that PTK-UR materials are highly tunable with properties that support their use in regenerative engineering applications.

CHAPTER 4: Ability for PTK-UR scaffolds to modulate cell behavior and facilitate cell growth

4.1 Introduction

The extracellular matrix (ECM) can be defined as the non-cellular component present within tissues that provides physical structure for cellular materials as well as initiates biochemical and biomechanical cues for morphogenesis, differentiation and homeostasis in tissues[96]. Therefore, when developing therapies to facilitate tissue regeneration, synthetic scaffolding is required to act as a temporary ECM in damaged tissues. Historically, tissue engineering systems have been relatively static scaffolds, but more recent development have turned to scaffolds that have topographical, mechanical, and biochemical properties that better mimic native ECM[97]. The addition of specific chemical moieties are used to create polymers with tunable properties for enhanced cell adhesion, crosslinking, and degradability[98]. Methods of scaffold fabrication include gas foaming, electrospinning, freeze-drying, solvent casting, and stereolithography[97,98].

Upon injury to the skin, the body elicits a wound healing response that develops a provisional ECM for the recruitment of inflammatory cells, endothelial cells, and fibroblasts before moving on to later stages of the wound healing process[99]. This inflammatory phase is characterized by an "oxidative burst" by inflammatory cells to prevent infection that is later reduced by the inherent antioxidant system of the skin[14]. However, chronic wounds tend to become stuck in the inflammatory phase, and a large influx of inflammatory cells results in an excessive production of reactive oxygen species that exceeds the reduction capacity of the skin antioxidant system and further damages skin ECM[100]. Therefore, there is a clinical need for synthetic skin ECM via tissue

engineering scaffolds that also provides antioxidant benefit to aid in the wound healing process in chronic wounds.

4.2 Materials and Methods

Materials

Cell culture reagents, including Dulbecco's Modified Eagle Medium (DMEM), fetal bovine serum (FBS), and penicillin/streptomycin were supplied by Gibco Cell Culture (Carlsbad, CA). The 2,2-diphenyl-1-picrylhydrazyl (DPPH) free radical was purchased from Fisher Scientific (Pittsburg, PA), and cell culture grade hydrogen peroxide was purchased from Sigma-Aldrich (Milwaukee, WI).

Cytotoxicity – Scaffold Extraction

Scaffold pieces at 100 mg/mL were incubated in Dulbecco's Modified Eagles Medium (DMEM) supplemented with 1% penicillin and streptomycin and 20% fetal bovine serum (FBS) for 24 hours at 37°C to produce material extracts. Extraction media was further diluted to 50 mg/mL in accordance with ISO10993 *in vitro* cytotoxicity testing. NIH 3T3 mouse fibroblast cells containing a GFP/luciferase reporter were seeded at 10,000 cells/well (n=4) in a 96-well plate for 24 hours. Cells were treated with 100 μL of extraction media and bioluminescence imaging with luciferin salt was used to measure viability at 24 hours after treatment using an *in vivo* imaging system (IVIS 200, Waltham, MA). Cell number was quantified via luminescence with respect to the no treatment control.

Antioxidant Capacity

The 2,2-diphenyl-1-picrylhydrazyl (DPPH) assay was used to evaluate the antioxidant activity of the PTK-UR scaffolds as previously described, with alterations[4].

10 mg scaffold pieces (n = 3) were treated with 2 mL of 200 μM DPPH solution in 80% ethanol/water at 37°C. DPPH radical was dissolved by vortexing vigorously for 30 min before the start of assay. Radical scavenging capacity was evaluated by absorbance at 517 nm compared to the DPPH negative control solution at 1 hr, 2 hr, 3 hr, 6 hr, 12 hr, 24 hr, and 36 hr. Antioxidant capacity is expressed as percent inhibition, calculated by Eq. 4.

$$\% \; Inhibition = \frac{A_c - A_s}{A_c}$$

Equation 11. Determination of antioxidant capacity of PTK-UR scaffolds.

In this equation, A_c is the absorbance of the DPPH control solution and A_s is the absorbance of the sample solution.

Cytoprotection

NIH 3T3 mouse fibroblast cells were seeded at a density of 10,000 cells/well in Dulbecco's Modified Eagles Medium (DMEM) supplemented with 10% FBS and 1% penicillin and streptomycin and allowed to adhere for 24 hours prior to treatment. PTK polyols of various masses were matched based on moles of thioketal bonds and crudely solubilized in 50 μM and 25 μM H_2O_2 culture media. 900t and 1500t were used as controls at a concentration of 0.5 mg/mL. Concentration for each polyol can be found in **Table A3**. Cells were treated with 200 μL of oxidative media containing polyols and incubated for 24 hours. Oxidative media without polyols was used as a control. Cell viability was measured at 24 hours on an *in vivo* imaging system (IVIS 200) using CellTiter-Glo Luminescent Cell Viability Assay (Promega, Madison, WI). Cell number was quantified via luminescence with respect to the no treatment control.

Statistics

All reported data are presented as the mean and standard deviation of the mean.

Statistical analysis was performed using single factor analysis of variance (ANOVA) and Tukey's multiple comparison tests, with p-values less than 0.05 being considered as statistically significant.

4.3 Results

Cytotoxicity

One method to evaluate cytotoxicity of the PTK-UR scaffold was to treat 2D cell cultures with material extracts in accordance with ISO 10993. Extracts at 50mg/mL were made by incubating scaffolds in media for 24 hours, and then using this media to treat cells for an additional 24 hours. Relative viability in comparison to a no treatment group was used to evaluate toxicity of any potential leachable materials. When treated with extracts, there was no significant reduction in cell viability compared to no treatment controls as seen in **Figure 10**. PEURs also did not show any reduction in cell viability following the extract treatment.

Cytotoxicity with Scaffold Extracts
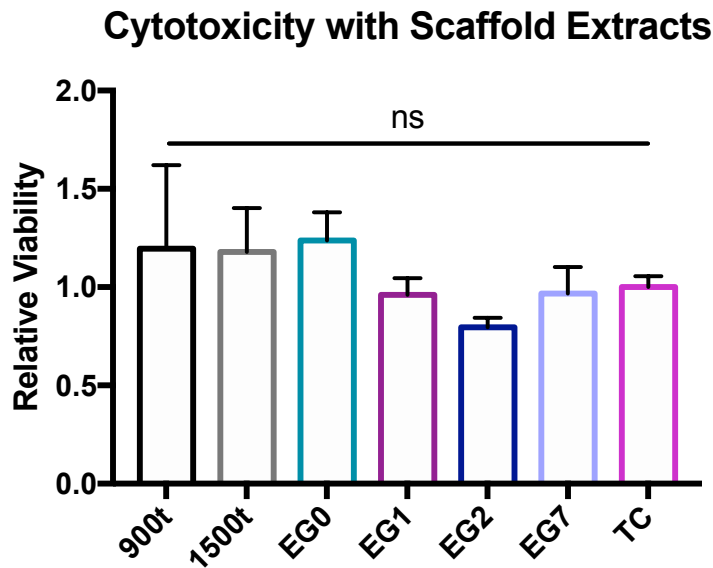
Figure 10. Cytotoxic effects of scaffold extracts *in vitro*. No significant decrease in cell viability was observed for cells treated with PEUR or PTK-UR scaffold extracts compared to tissue culture controls.

Antioxidant Activity and Cell Protective Ability of PTK-UR Polymers

The 1,1-diphenyl-2-picrylhydrazyl (DPPH) assay was used to measure the antioxidant capacity of PTK-UR and PEUR scaffolds over 36 hours. PTK-UR scaffolds readily reduced environmental DPPH radicals in solution, while PEUR scaffolds scavenged little to no radicals from the solution. **Figure 11A** shows the most hydrophilic scaffolds, EG1, EG2 and EG7, scavenged the greatest amount of DPPH radicals, 92%, 92%, and 87%, respectively, by hour 36. PEUR scaffolds had little scavenging effect, with only 31% and 36% of radicals scavenged by hour 36 for 900t and 1500t scaffolds.
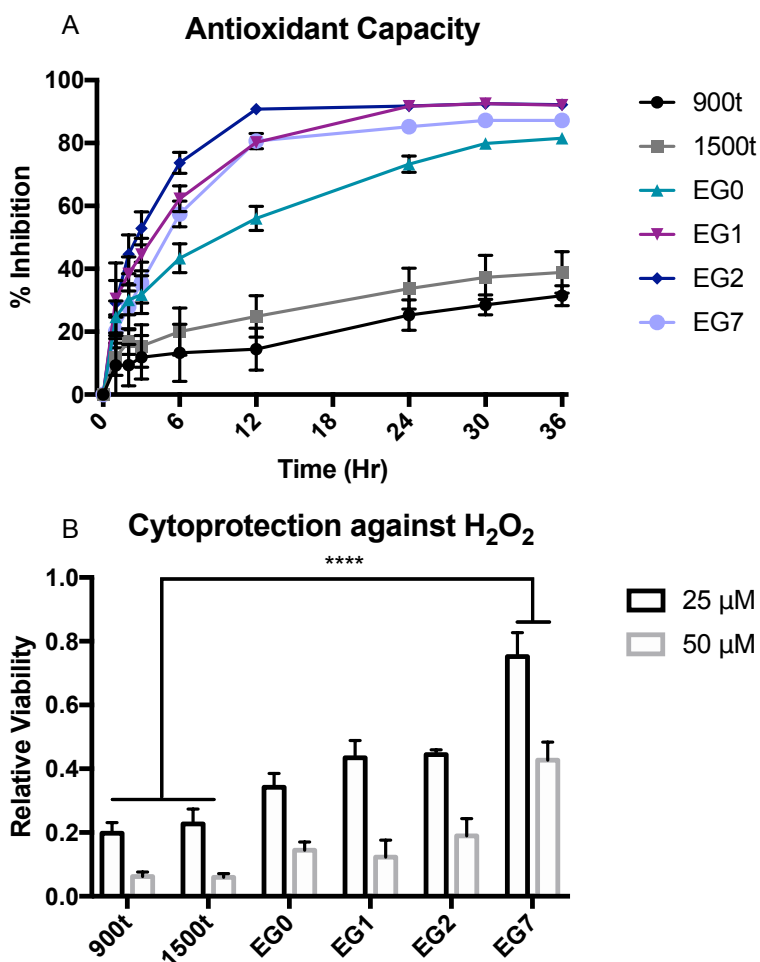
Figure 11. Antioxidant effects of PTK-UR and PEUR formulations. (A) DPPH assay evaluating ROS scavenging capacity of scaffolds. (B) Cytoprotection assay evaluating protective benefit of polyols *in vitro* with cell cultures treated with 25μM and 50μM hydrogen peroxide, *$p < 0.05$.

The ability for PTK polymers to provide a protective benefit for cells *in vitro* was evaluated by treating NIH 3T3 fibroblast cells with oxidative media containing crudely solubilized polymer matched based on moles of TK bonds of each respective polymer, and measuring cell viability after 24 hours. **Figure 11B** shows EG7 provided the most significant protective benefit, with nearly 40% and 75% of cells remaining viable in the 50 μM treatment group and 25 μM treatment group, respectively, compared to cells treated with other less hydrophilic PTK and PEUR diols.

4.4 Discussion

The most important aspect in the design and implementation of biomaterials in the body is biocompatibility. That is, the material is able to coexist with natural tissues without causing adverse effects[101]. This includes host reactions to both the material as well as degradation products released from the system. Updated definitions of biocompatibility not only require the material to elicit a minimal host response, but also include the notion of bioactivity, in which the material induces a specific desired response from the tissue[102]. These bioactive features can be fine-tuned into the system and include promotion of tissue ingrowth, stimuli-responsive degradation, or antioxidant effects of the biomaterial. Specifically, antioxidant activity of biomaterials or biomaterial constituents such as polyphenols, curcumin, as well as synthetic chemical moieties have shown to promote tissue regeneration in variety of diseases that exhibit oxidative stress as one of their main pathologies including wound healing, atherosclerosis, and cardiovascular disease[103–105]. Tissue engineering systems must have tunable properties to not only be biologically inert but also be biologically active to promote regeneration of tissues.

Often, the first step in determining the biocompatibility is evaluating the *in vitro* cytocompatibility of a biomaterial in 2D or 3D cell culture according to ISO 10993 standards[106]. Treating 2D cell cultures with material extracts is one way to measure the cytotoxicity of any leachable products from the biomaterial. Here, PEUR and PTK-UR scaffolds were incubated in cell culture media for 24 hours to create extracts at 50mg/mL, and then cells were treated with the extraction media. After 24 hours, no significant decreases in cell viability were seen for PEUR or PTK-UR extracts compared to no treatment controls. Additionally, 3D culture on top of scaffolds can measure cells ability to stick and lay down ECM proteins in the provisional matrix.

Chronic wound healing capabilities are often compromised by the excessive production of reactive oxygen species, which can lead to cytotoxic injury and cellular damage to surrounding tissue[15,48]. Therefore, treatments that have antioxidant properties to reduce environmental ROS in chronic wounds are desirable[48]. Scaffolds in the EG series presented here not only are degraded by cell-produced ROS, but also scavenge free radicals from the environment. The 1,1-diphenyl-2-picrylhydrazyl (DPPH) assay utilizes the DPPH free radical to measure the scavenging ability of materials with antioxidant properties, and when reduced, the solution will change from purple to yellow[107]. The degree of scavenging is then measured by absorbance. PTK-UR scaffolds with increased hydrophilicity were better able to scavenge DPPH free radicals from the solution over 36 hours. Similarly to the increased degradation kinetics with increased PEG content, high swelling ratio of EG scaffolds allows for more exposure of TK bonds in the matrix, resulting in radicals being reduced by these antioxidant linkages. Interestingly, EG1 and EG2 scaffolds appear to more readily than EG7. However, in order to keep molecular

weight of the polymers similar, as PEG increases in the PTK diols the number of TK bonds per mole decreases. In the DPPH assay, scaffolds were mass matched, so lower EG scaffolds contained more TK bonds, while EG7 contained the least number of TK bonds (**Table B1**). When data is extrapolated, it can be shown that although EG1 and EG2 appear to perform between EG7 actually is able to scavenge the most DPPH per mole of polymer (**Figure B1**).

The ability of the PTK-UR scaffolds to scavenge ROS from the environment also provides a protective benefit to cells *in vitro*. When treated with cell media containing hydrogen peroxide and PEUR or PTK-UR polyols, cells had higher viability after 24 hours after being treated with more hydrophilic polyols compared to less hydrophilic PTKs and PEURs. The ability for PTK-UR diols and scaffolds to reduce radicals in vitro and protect cells provide insight on how the scaffolds will behave in vivo and provide additional benefits to facilitate cell growth and tissue regeneration.

4.5 Conclusion

The biocompatibility and ability for materials to modulate cell behavior is a key feature that must be at the forefront of the design of tissue engineering scaffolds. Additionally, although a material may not present any cytotoxic affects to cells, but if the material is also not bioactive there will be limited cell infiltration and tissue regeneration. Here it is shown that a family of poly(thio ketal) urethane biomaterials do not have any cytotoxic affects from constituents that may leach out in an aqueous environment. These novel materials also prove to have an antioxidant effect in the presence of free radicals, and provide a protective benefit for cells *in vitro* in comparison to conventional polyester polymers. When exposed to ROS in media, PTKs, notably EG7, are able to scavenge

oxidants from the media and enhance cell viability. *In vitro* investigation shows that cells not only remain viable in the presence of PTK-UR scaffolds, but also can be protected by damaging ROS in the environment.

CHAPTER 5: Summary and future directions

5.1 Synopsis

The chronic wound industry amounts to $25 billion yearly, with diabetic foot ulcers affecting 6.5 million people every year[2]. With the growing incidence of chronic wounds, therapies that address their pathologies are needed to treat these patients. Although biodegradable treatments options are currently available on the market, they are often fabricated from expensive materials, and these materials have shown to have degradation kinetics that do not match up with the rate of tissue regeneration. Additionally, hydrolytic degradation mechanisms of available products can become autocatalytic and cause further damage to the regenerating tissue. Here, poly(thio ketal) urethane biomaterials are inexpensively synthesized and selectively degraded by cell-mediated mechanisms that are present in the chronic wound microenvironment. Material properties of the resulting scaffolds are highly tunable to allow for optimal tissue regeneration in chronic wounds.

In Aim 1, the characterization of a library of poly(thio ketal) polymers was done to understand how the hydrophilic/hydrophobic balance of the polymer diols and subsequent porous scaffolds affected their material properties. The PTK-UR materials were evaluated against conventional polyester urethane biomaterials that have been thoroughly investigated in past research. In PTK-UR materials, an increase in PEG content in the diol monomers increases their hydrophilicity, while it does not cause a significant change the mechanical properties of the scaffolds compared to PEURs. An increase in hydrophilicity consequently increases the degree of swelling in aqueous

55

conditions, which allows for more exposure of ROS-responsive thioketal bonds that can be broken down by hydroxyl radicals, leading to more rapid scaffold degradation in a dose-dependent manner.

In Aim 2, the ability of the PTK-UR scaffolds to modulate cell behavior and facilitate cell growth was evaluated. When treated with scaffold extraction media, no significant reduction in cell viability was observed *in vitro*. This implies that any leachable materials that may come from the scaffold under aqueous conditions are not toxic to cells. Not only do PTK-UR scaffolds degrade in the presence of reactive oxygen species, but they also scavenge ROS from the environment in a manner related to the moles of thioketal bonds present in each respective monomer as shown in the DPPH assay. As with the degradation kinetics, increased hydrophilicity increases the exposure of TK bonds that are able to scavenge ROS. This antioxidant effect enhances cell viability *in vitro* when cells are cultured in an oxidative environment.

All in all, these tunable properties of PTK-UR biomaterials make them an attractive candidate for wound healing treatments and they prove to be a promising new class of biomaterials for tissue engineering. Investigation into *in vivo* animal models and the use of these scaffolds as drug delivery systems will provide further insight into the efficacy of these scaffolds for chronic wound healing.

5.2 Concerns and limitations

The PTK-UR biomaterials presented here were evaluated for *in vitro* cytotoxicity with a single cell line. Although these experiments provide insight on the toxicity of any leachable materials and the ability for cells to remain viable in the presence of the scaffolds, they do not evaluate the immune response the scaffolds could illicit *in vivo*. It

is important to note the potential immune response when translating the material into the clinical environment. However, appropriate *in vitro* analysis and advanced animal models can easily overcome this hurdle to analyze these effects.

The PTK-UR polyols and scaffolds used here are made in small batches, and their formulation is easily controllable due to the scale. By making both polymer and scaffolds on a small scale, scaffold production is low-throughput and batch-to-batch variability can be seen in the fabrication of scaffold batches that remain unvarying in their composition and morphology. Translation of this biomaterial for clinical application in wound healing would require scale up of production and manufacturing, which could present a challenge in maintaining consistency between large batches of the product. To overcome this obstacle, a team of trained and knowledgeable engineers could design a high-throughput production system to produce polymer and scaffolds whose properties remain consistent across lots.

5.3 Future Directions

The work presented here involves *in vitro* characterization of the biomaterial, so the next step is to evaluate the effects of the scaffolds in *in vivo* animal models. In efforts to validate the wound healing effects *in vivo*, other members of the Duvall lab at Vanderbilt University have conducted porcine wound healing models to evaluate immune response, fibrotic tissue formation, and wound closure. Porcine models are chosen over rodent models because porcine skin is a better representation of human skin. Therefore, these models will provide better insight into host response to hypothesize the effects following translation to the clinical setting.

Ongoing work with PTK-UR scaffolds strives to achieve the long-term goal of using the system to deliver siRNA therapeutics to chronic wound environments to further enhance the wound healing capabilities of non-healing wounds. Key genes that have shown to be affected in chronic wounds are HIF-1α and PHD2. HIF-1α is stabilized in hypoxic conditions and dimerizes with HIF-1β, and is then degraded by PHD2 upon restoration of normoxia[108,109]. In chronic wounds, especially diabetic ulcers, HIF-1α is destabilized despite the hypoxic environment of the wound, leading to its degradation by PHD2. This results in a decrease in the production of growth factors required for effective wound healing, such as vascular endothelial growth factor (VEGF), platelet-derived growth factor (PDGF), stromal cell factor-1 (SDF-1) and fibroblast growth factor 2 (FGF-2), among others[3,57]. It has been shown that by silencing PHD2 in the chronic wound microenvironment, the upregulation if the growth factors can promote healing[57,110]. The goal of the PTK-UR system presented here is to deliver the therapeutic by covalently bonding amine-modified siRNA within the foam matrix. The siRNA will subsequently be release upon oxidative degradation of the scaffolds.

5.4 Broader Impacts

Future work described in section 5.3 outlines how PTK-UR materials will be evaluated in animal models as well as evaluated as drug delivery devices for siRNA therapeutics. This material has the potential to be translated to the clinic and undergo clinical trials either alone or as a drug delivery vehicle for siRNA therapeutics. Currently on the market, Integra® and NovoSorb™ are considered the gold standard for chronic wound treatment. However, Integra® can be quite expensive, as it is fabricated from naturally occurring polymers which intrinsically can be costly[26]. NovoSorb™ is a

synthetic matrix, making it more inexpensive compared to natural polymers. However, NovoSorb[TM] is biodegradable only via hydrolysis, making it a slower degradation process and also introducing the possibility of autocatalytic degradation[33]. The increased hydrophilicity of PTK-UR materials allows for better wound exudate absorption, which keeps the wound environment moist. Additionally, the availability of a biodegradable wound dressing that does not contain drug component also will likely have a less rigorous regulatory process, which accelerates its movement to market and decreases approval costs.

CHAPTER 6: Conclusion

The design of biomaterials that are biodegradable via cell-mediated degradation, biocompatible, and possess favorable material properties that can be tailored to the specific tissue application is a rapidly growing filed in biomedical engineering and regenerative medicine. The PTK-UR scaffolds presented here can be affordably synthesized and possess properties that can enhance the healing outcomes for patients with chronic wounds.

Bibliography

1. Guo, S. & DiPietro, L. A. Factors affecting wound healing. *J. Dent. Res.* **89**, 219–229 (2010).

2. Han, G. & Ceilley, R. Chronic Wound Healing: A Review of Current Management and Treatments. *Adv. Ther.* **34**, 599–610 (2017).

3. Bharara, M., et al. *et al.* Disturbed hypoxic responses as a pathogenic mechanism of diabetic foot ulcers. *Diabetes. Metab. Res. Rev.* **28**, 3–12 (2009).

4. Martin, J. R. *et al.* A porous tissue engineering scaffold selectively degraded by cell-generated reactive oxygen species. *Biomaterials* **35**, 3766–3776 (2014).

5. Hunt, T. K., Hopf, H. & Hussain, Z. Physiology of wound healing. *Adv. Skin Wound Care* **13**, 6–11 (2000).

6. Cañedo-Dorantes, L. & Cañedo-Ayala, M. Skin acute wound healing: A comprehensive review. *Int. J. Inflam.* **2019**, (2019).

7. Velnar, T., Bailey, T. & Smrkolj, V. The wound healing process: An overview of the cellular and molecular mechanisms. *J. Int. Med. Res.* **37**, 1528–1542 (2009).

8. Harding, K. G. Science, medicine, and the future: Healing chronic wounds. *Bmj* **324**, 160–163 (2002).

9. Krzyszczyk, P., Schloss, R., Palmer, A. & Berthiaume, F. The role of macrophages in acute and chronic wound healing and interventions to promote pro-wound healing phenotypes. *Front. Physiol.* **9**, 1–22 (2018).

10. Nour, S. *et al.* A review of accelerated wound healing approaches: biomaterial-assisted tissue remodeling. *J. Mater. Sci. Mater. Med.* **30**, (2019).

11. Falanga, V. The chronic wound: Impaired healing and solutions in the context of wound bed preparation. *Blood Cells, Mol. Dis.* **32**, 88–94 (2004).

12. Demidova-Rice, T. N. T. N., Hamblin, M. R. M. R. & Herman, I. . I. M. Acute and Impaired Wound Healing: Pathophysiology and Current Methods for Drug Delivery, Part 1: Normal and Chronic Wounds: Biology, Causes, and Approaches to Care. *Adv. Ski. wound care* **25**, 304–314 (2012).

13. Schäfer, M. & Werner, S. Oxidative stress in normal and impaired wound repair. *Pharmacol. Res.* **58**, 165–171 (2008).

14. Kanta, J. The role of hydrogen peroxide and other reactive oxygen species in wound healing. *Acta Medica (Hradec Kralove)* **54**, 97–101 (2011).

15. Mustoe, T. A., O'Shaughnessy, K. & Kloeters, O. Chronic wound pathogenesis and current treatment strategies: A unifying hypothesis. *Plast. Reconstr. Surg.* **117**, 35–41 (2006).

16. Ke, Q. & Costa, M. Hypoxia-Inducible Factor-1 (HIF-1). **70**, 1469–1480 (2006).

17. Déry, M. A. C., Michaud, M. D. & Richard, D. E. Hypoxia-inducible factor 1: Regulation by hypoxic and non-hypoxic activators. *Int. J. Biochem. Cell Biol.* **37**, 535–540 (2005).

18. Jones, V., Grey, J. E. & Harding, K. G. ABC of wound healing: Wound dressings. *Br. Med. J.* **332**, 777–780 (2006).

19. Fleck, C. A. Why 'Wet to Dry'? *J. Am. Col. Certif. Wound Spec.* **1**, 109–113 (2009).

20. Kamoun, E. A., Kenawy, E. R. S. & Chen, X. A review on polymeric hydrogel membranes for wound dressing applications: PVA-based hydrogel dressings. *J.*

Adv. Res. **8**, 217–233 (2017).

21.   Dabiri, G., Damstetter, E. & Phillips, T. Choosing a Wound Dressing Based on Common Wound Characteristics. *Adv. Wound Care* **5**, 32–41 (2016).

22.   Saghazadeh, S. *et al.* Drug Delivery Systems and Materials for Wound Healing Applications. 138–166 (2019). doi:10.1016/j.addr.2018.04.008.Drug

23.   Wong, V. W. & Gurtner, G. C. Tissue engineering for the management of chronic wounds: Current concepts and future perspectives. *Exp. Dermatol.* **21**, 729–734 (2012).

24.   Hu, M. S. *et al.* Tissue engineering and regenerative repair in wound healing. *Ann. Biomed. Eng.* **42**, 1494–1507 (2014).

25.   Shi, L. & Ronfard, V. Biochemical and biomechanical characterization of porcine small intestinal submucosa (SIS): a mini review. *Int. J. Burns Trauma* **3**, 173–9 (2013).

26.   Greenwood, J. E. *Hybrid Biomaterials for Skin Tissue Engineering. Skin Tissue Engineering and Regenerative Medicine* (Elsevier Inc., 2016). doi:10.1016/B978-0-12-801654-1.00010-3

27.   Johnson, N. & Wang, Y. Drug Delivery Systems for Wound Healing. *Curr. Pharm. Biotechnol.* **16**, 621–629 (2015).

28.   Barrientos, S., Brem, H., Stojadinovic, O. & Tomic-Canic, M. Clinical application of growth factors and cytokines in wound healing. *Wound Repair Regen.* **22**, 569–578 (2014).

29.   Mustoe, T. Understanding chronic wounds: A unifying hypothesis on their pathogenesis and implications for therapy. *Am. J. Surg.* **187**, S65–S70 (2004).

30. Selvaraj Dhivya, Viswanadha Vijaya Padmab, E. S. Wound dressings – a review. *BioMedicine* **5**, 24–28 (2015).

31. Eaglstein, W. H. Experiences with biosynthetic dressings. *J. Am. Acad. Dermatol.* **12**, 434–440 (1985).

32. Williams, C. Allevyn. *Br. J. Nurs.* **4**, 107–110 (1995).

33. Li, A., Dearman, B. L., Crompton, K. E., Moore, T. G. & Greenwood, J. E. Evaluation of a novel biodegradable polymer for the generation of a dermal matrix. *J. Burn Care Res.* **30**, 717–728 (2009).

34. Kaiser, D., Hafner, J., Mayer, D., French, L. E. & Läuchli, S. Alginate dressing and polyurethane film versus paraffin gauze in the treatment of split-thickness skin graft donor sites: A randomized controlled pilot study. *Adv. Ski. Wound Care* **26**, 67–73 (2013).

35. Sood, A., Granick, M. S. & Tomaselli, N. L. Wound Dressings and Comparative Effectiveness Data. *Adv. Wound Care* **3**, 511–529 (2014).

36. Draye, J. P. *et al.* In vitro and in vivo biocompatibility of dextran dialdehyde cross-linked gelatin hydrogel films. *Biomaterials* **19**, 1677–1687 (1998).

37. Nyame, T. T., Chiang, H. A., Leavitt, T., Ozambela, M. & Orgill, D. P. Tissue-Engineered Skin Substitutes. *Plast. Reconstr. Surg.* **136**, 1379–1388 (2015).

38. Gun'Ko, V. M. *et al.* Characterisation and performance of hydrogel tissue scaffolds. *Soft Matter* **6**, 5351–5358 (2010).

39. Callcut, R. A., Schurr, M. J., Sloan, M. & Faucher, L. D. Clinical experience with Alloderm: A one-staged composite dermal/epidermal replacement utilizing processed cadaver dermis and thin autografts. *Burns* **32**, 583–588 (2006).

40. MacEwan, M. R. *et al.* Comparison of a Fully Synthetic Electrospun Matrix to a Bi-Layered Xenograft in Healing Full Thickness Cutaneous Wounds in a Porcine Model. *Cureus* **9**, 1–10 (2017).

41. MacEwan, M. R., MacEwan, S., Kovacs, T. R. & Batts, J. What Makes the Optimal Wound Healing Material? A Review of Current Science and Introduction of a Synthetic Nanofabricated Wound Care Scaffold. *Cureus* **9**, (2017).

42. Halliwell, B. How to characterize a biological antioxidant. *Free Radic. Res.* **9**, 1–32 (1990).

43. Halliwell, B., Aeschbach, R., Löliger, J. & Aruoma, O. I. The characterization of antioxidants. *Food Chem. Toxicol.* **33**, 601–617 (1995).

44. Huang, D., Boxin, O. U. & Prior, R. L. The chemistry behind antioxidant capacity assays. *J. Agric. Food Chem.* **53**, 1841–1856 (2005).

45. RS, B., DG, C., Prakash Reddy, K. S. & Shivaji. A Review of Antioxidants. *J. Indian Acad. Oral Med. Radiol.* **23**, S351–S353 (2011).

46. Lü, J. M., Lin, P. H., Yao, Q. & Chen, C. Chemical and molecular mechanisms of antioxidants: Experimental approaches and model systems. *J. Cell. Mol. Med.* **14**, 840–860 (2010).

47. Xu, Z., Han, S., Gu, Z. & Wu, J. Advances and Impact of Antioxidant Hydrogel in Chronic Wound Healing. *Adv. Healthc. Mater.* **9**, 1–11 (2020).

48. Baek, J. & Lee, M. G. Oxidative stress and antioxidant strategies in dermatology. *Redox Rep.* **21**, 164–169 (2016).

49. Masaki, H. Role of antioxidants in the skin: Anti-aging effects. *J. Dermatol. Sci.* **58**, 85–90 (2010).

50.   Novo, E. & Parola, M. Redox mechanisms in hepatic chronic wound healing and
        fibrogenesis. *Fibrogenes. Tissue Repair* **1**, 1–58 (2008).

51.   Xu, Q., He, C., Xiao, C. & Chen, X. Reactive Oxygen Species (ROS) Responsive
        Polymers for Biomedical Applications. *Macromol. Biosci.* **16**, 635–646 (2016).

52.   Lee, J. Y. *et al.* Design of a 3D BMP-2-delivering tannylated PCL scaffold and its
        anti-oxidant, anti-inflammatory, and osteogenic effects in vitro. *Int. J. Mol. Sci.* **19**,
        (2018).

53.   Marino, A. *et al.* Gelatin/nanoceria nanocomposite fibers as antioxidant scaffolds
        for neuronal regeneration. *Biochim. Biophys. Acta - Gen. Subj.* **1861**, 386–395
        (2017).

54.   Li, J. *et al.* An anti-oxidative and conductive composite scaffold for cardiac tissue
        engineering. *Compos. Part B Eng.* **199**, (2020).

55.   van Lith, R., Gregory, E. K., Yang, J., Kibbe, M. R. & Ameer, G. A. Engineering
        biodegradable polyester elastomers with antioxidant properties to attenuate
        oxidative stress in tissues. *Biomaterials* **35**, 8113–8122 (2014).

56.   Yao, Y. *et al.* ROS-responsive polyurethane fibrous patches loaded with
        methylprednisolone (MP) for restoring structures and functions of infarcted
        myocardium in vivo. *Biomaterials* **232**, (2020).

57.   Martin, J. R. *et al.* Local Delivery of PHD2 siRNA from ROS-Degradable
        Scaffolds to Promote Diabetic Wound Healing. *Adv. Healthc. Mater.* **5**, 2751–
        2757 (2016).

58.   Wells, C. M. *et al.* Stimuli-responsive drug release from smart polymers. *J. Funct.
        Biomater.* **10**, (2019).

59.   CHATTERJEE;, S. & HUI, P. C. Review of Stimuli-Responsive Polymers in
       Delivery and Textile Application. *Molecules* (2019).
       doi:10.3390/molecules24142547

60.   Saravanakumar, G., Kim, J. & Kim, W. J. Reactive-Oxygen-Species-Responsive
       Drug Delivery Systems: Promises and Challenges. *Adv. Sci.* **4**, (2017).

61.   Bawa, P., Pillay, V., Choonara, Y. E. & Du Toit, L. C. Stimuli-responsive
       polymers and their applications in drug delivery. *Biomed. Mater.* **4**, (2009).

62.   De las Heras Alarcón, C., Pennadam, S. & Alexander, C. Stimuli responsive
       polymers for biomedical applications. *Chem. Soc. Rev.* **34**, 276–285 (2005).

63.   Gandhi, A., Paul, A., Sen, S. O. & Sen, K. K. Studies on thermoresponsive
       polymers: Phase behaviour, drug delivery and biomedical applications. *Asian J.
       Pharm. Sci.* **10**, 99–107 (2015).

64.   Tao, W. & He, Z. ROS-responsive drug delivery systems for biomedical
       applications. *Asian J. Pharm. Sci.* **13**, 101–112 (2018).

65.   Zhu, Y. J. & Chen, F. pH-Responsive Drug-Delivery Systems. *Chem. - An Asian J.*
       10, 284–305 (2015).

66.   Bikram, M. & West, J. L. Thermo-responsive systems for controlled drug delivery.
       Expert Opin. Drug Deliv. **5**, 1077–1091 (2008).

67.   Hu, J., Zhang, G. & Liu, S. Enzyme-responsive polymeric assemblies,
       nanoparticles and hydrogels. *Chem. Soc. Rev.* **41**, 5933–5949 (2012).

68.   D. Scott Wilson, Guillaume Dalmasso, Lixin Wang, Shanthi V. Sitaraman, Didier
       Merlin, and N. M. Orally delivered thioketal-nanoparticles loaded with TNFα-
       siRNA target inflammation and inhibit gene expression in the intestines. *Bone* **23**,

1–7 (2008).

69.   Gupta, M. K. *et al.* Cell protective, ABC triblock polymer-based thermoresponsive hydrogels with ROS-triggered degradation and drug release. *J. Am. Chem. Soc.* **136**, 14896–14902 (2014).

70.   Gupta, M. K., Martin, J. R., Dollinger, B. R., Hattaway, M. E. & Duvall, C. L. Thermogelling, ABC Triblock Copolymer Platform for Resorbable Hydrogels with Tunable, Degradation-Mediated Drug Release. *Adv. Funct. Mater.* **27**, 1–14 (2017).

71.   Patil, P. *et al.* Porcine Ischemic Wound-Healing Model for Preclinical Testing of Degradable Biomaterials. *Tissue Eng. - Part C Methods* **23**, 754–762 (2017).

72.   Godavitarne, C., Robertson, A., Peters, J. & Rogers, B. Biodegradable materials. *Orthop. Trauma* **31**, 316–320 (2017).

73.   Wang, M., Chen, L. J., Ni, J., Weng, J. & Yue, C. Y. Manufacture and evaluation of bioactive and biodegradable materials and scaffolds for tissue engineering. *J. Mater. Sci. Mater. Med.* **12**, 855–860 (2001).

74.   Liu, X., Holzwarth, J. M. & Ma, P. X. Functionalized Synthetic Biodegradable Polymer Scaffolds for Tissue Engineering. *Macromol. Biosci.* **12**, 911–919 (2012).

75.   Guo, B. & Ma, P. X. Synthetic biodegradable functional polymers for tissue engineering: A brief review. *Sci. China Chem.* **57**, 490–500 (2014).

76.   Izquierdo, R. *et al.* Biodegradable PCL scaffolds with an interconnected spherical pore network for tissue engineering. *J. Biomed. Mater. Res. - Part A* **85**, 25–35 (2008).

77.   Oh, S. H., Park, I. K., Kim, J. M. & Lee, J. H. In vitro and in vivo characteristics

of PCL scaffolds with pore size gradient fabricated by a centrifugation method. *Biomaterials* **28**, 1664–1671 (2007).

78. Pattison, M. A., Wurster, S., Webster, T. J. & Haberstroh, K. M. Three-dimensional, nano-structured PLGA scaffolds for bladder tissue replacement applications. *Biomaterials* **26**, 2491–2500 (2005).

79. Ren, T., Ren, J., Jia, X. & Pan, K. The bone formation in vitro and mandibular defect repair using PLGA porous scaffolds. *J. Biomed. Mater. Res. - Part A* **74**, 562–569 (2005).

80. Gogolewski, S., Gorna, K. & Turner, A. S. Regeneration of bicortical defects in the iliac crest of estrogen-deficient sheep, using new biodegradable polyurethane bone graft substitutes. *J. Biomed. Mater. Res. Part A* **79**, 963–73 (2006).

81. Hafeman, A. E. *et al.* Injectable biodegradable polyurethane scaffolds with release of platelet-derived growth factor for tissue repair and regeneration. *Pharm. Res.* **25**, 2387–2399 (2008).

82. Santerre, J. P., Woodhouse, K., Laroche, G. & Labow, R. S. Understanding the biodegradation of polyurethanes: From classical implants to tissue engineering materials. *Biomaterials* **26**, 7457–7470 (2005).

83. Guelcher, S. *et al.* Synthesis, in vitro degradation, and mechanical properties of two-component poly (ester urethane)urea scaffolds: Effects of water and polyol composition. *Tissue Eng.* **13**, 2321–2333 (2007).

84. Hafeman, A. E. *et al.* Characterization of the Degradation Mechanisms of Lysine-derived Aliphatic Poly(ester urethane) Scaffolds. *Biomaterials* **32**, 419–429 (2011).

85. Zeimaran, E. *et al.* Self-Healing Polyester Urethane Supramolecular Elastomers Reinforced with Cellulose Nanocrystals for Biomedical Applications. *Macromol. Biosci.* **19**, 1–12 (2019).

86. Bil, M., Mrówka, P., Kołbuk, D. & Święszkowski, W. Multifunctional composite combining chitosan microspheres for drug delivery embedded in shape memory polyester-urethane matrix. *Compos. Sci. Technol.* **201**, 1–9 (2021).

87. Helminen, A., Kylmä, J., Tuominen, J. & Seppälä, J. V. Effect of structure modification on rheological properties of biodegradable poly(ester-urethane). *Polym. Eng. Sci.* **40**, 1655–1662 (2000).

88. Laschke, M. W. *et al.* In vivo biocompatibility and vascularization of biodegradable porous polyurethane scaffolds for tissue engineering. *Acta Biomater.* **5**, 1991–2001 (2009).

89. Dumas, J. E. *et al.* Balancing the rates of new bone formation and polymer degradation enhances healing of weight-bearing allograft/polyurethane composites in rabbit femoral defects. *Tissue Eng. - Part A* **20**, 115–129 (2014).

90. Schollenberger, C. S. & Stewart, F. D. Thermoplastic polyurethane hydrolysis stability. *Die Angew. Makromol. Chemie* **29**, 413–430 (1973).

91. Gorna, K. & Gogolewski, S. Preparation, degradation, and calcification of biodegradable polyurethane foams for bone graft substitutes. *J. Biomed. Mater. Res. - Part A* **67**, 813–827 (2003).

92. Wandel, M. B. *et al.* Concomitant control of mechanical properties and degradation in resorbable elastomer-like materials using stereochemistry and stoichiometry for soft tissue engineering. *Nat. Commun.* **12**, 1–13 (2021).

93. Mir, M. *et al.* Synthetic polymeric biomaterials for wound healing: a review. *Prog. Biomater.* **7**, 1–21 (2018).

94. Çakmak, E. G., Dalgakiran, D. & Güner, F. S. Castor oil and PEG-based shape memory polyurethane films: effect of chain extender amount on some polymer properties and performance. *Turkish J. Chem.* **42**, 1161–1173 (2018).

95. Chumakov, A., Batalova, V. & Slizhov, Y. Electro-Fenton-like reactions of transition metal ions with electrogenerated hydrogen peroxide. *AIP Conf. Proc.* **1772**, (2016).

96. Frantz, C., Stewart, K. M. & Weaver, V. M. The extracellular matrix at a glance. *J. Cell Sci.* **123**, 4195–4200 (2010).

97. Wade, R. J. & Burdick, J. A. Engineering ECM signals into biomaterials. *Mater. Today* **15**, 454–459 (2012).

98. Eltom, A., Zhong, G. & Muhammad, A. Scaffold Techniques and Designs in Tissue Engineering Functions and Purposes: A Review. *Adv. Mater. Sci. Eng.* **2019**, (2019).

99. Agren, M. S. & Werthen, M. The Extracellular Matrix in Wound Healing: A Closer Look at Therapeutics for Chronic Wounds. *Int. J. Low. Extrem. Wounds* **6**, 82–97 (2007).

100. Zhao, R., Liang, H., Clarke, E., Jackson, C. & Xue, M. Inflammation in chronic wounds. *Int. J. Mol. Sci.* **17**, 1–14 (2016).

101. Williams, D. F. On the mechanisms of biocompatibility. *Biomaterials* **29**, 2941–2953 (2008).

102. Bernard, M., Jubeli, E., Pungente, M. D. & Yagoubi, N. Biocompatibility of

polymer-based biomaterials and medical devices-regulations,: In vitro screening and risk-management. *Biomater. Sci.* **6**, 2025–2053 (2018).

103.   Shavandi, A. *et al.* Polyphenol uses in Biomaterials Engineering. 91–106 (2019). doi:10.1016/j.biomaterials.2018.03.018.Polyphenol

104.   Ahangari, N. *et al.* Curcumin in tissue engineering: A traditional remedy for modern medicine. *BioFactors* **45**, 135–151 (2019).

105.   Martin, J. R., Patil, P., Yu, F., Gupta, M. K. & Duvall, C. L. Enhanced stem cell retention and antioxidative protection with injectable, ROS-degradable PEG hydrogels. *Biomaterials* **263**, 120377 (2020).

106.   Devi, N. & Dutta, J. Biological Evaluation of Medical Devices Part 5: Tests for in vitro cytotoxicity (ISO 10993-5). *Int. Stand.* **3**, (2009).

107.   Sanna, D., Delogu, G., Mulas, M., Schirra, M. & Fadda, A. Determination of Free Radical Scavenging Activity of Plant Extracts Through DPPH Assay: An EPR and UV-Vis Study. *Food Anal. Methods* **5**, 759–766 (2012).

108.   Chandela, A. & Ueno, Y. Systemic delivery of small interfering RNA therapeutics: Obstacles and advances. *Rev. Agric. Sci.* **7**, 10–28 (2019).

109.   Tokatlian, T. & Segura, T. siRNA applications in nanomedicine. *Wiley Interdiscip. Rev. Nanomedicine Nanobiotechnology* **2**, 305–315 (2010).

110.   Nelson, C. E. *et al.* Tunable delivery of sirna from a biodegradable scaffold to promote angiogenesis in vivo. *Adv. Mater.* **26**, 607–614 (2014).

APPENDIX A: Chapter 3 Supplementary Information

	900t (900 Da)	1500t (1500 Da)	EG0 (2000 Da)	EG1 (2000 Da)	EG2 (2000 Da)	EG7 (2000 Da)
Polyol	100	100	100	100	100	100
Water	1.50	1.50	1.50	1.50	1.50	0.50
TEGOAMIN 33	2.3	2.3	2.3	2.3	2.3	2.3
Turkey Red Oil	1.00	1.00	1.00	1.00	1.00	0.50
Calcium Stearate	4.0	4.0	4.0	4.0	4.0	4.0
LTI	51.8	38	27.6	27.6	27.6	16.1

Table A1. Parts per hundred parts polyol (PPHP) for scaffold components for each polyol. Values shown for PTK diols are for 2000 Da polymers, while 900t and 1500t are 900 Da and 1500 Da, respectively.

	900t (900 Da)	1500t (1500 Da)	EG0 (2000 Da)	EG1 (2000 Da)	EG2 (2000 Da)	EG7 (2000 Da)
Polyol	100	100	100	100	100	100
Bismuth Neodecanoate	2.5	2.5	2.5	2.5	5.0	2.5
LTI	34.5	20.7	10.4	10.4	10.4	10.4

Table A2. Parts per hundred parts polyol (PPHP) for film components for each polyol. Values shown for PTK diols are for 2000 Da polymers, while 900t and 1500t are 900 Da and 1500 Da, respectively.
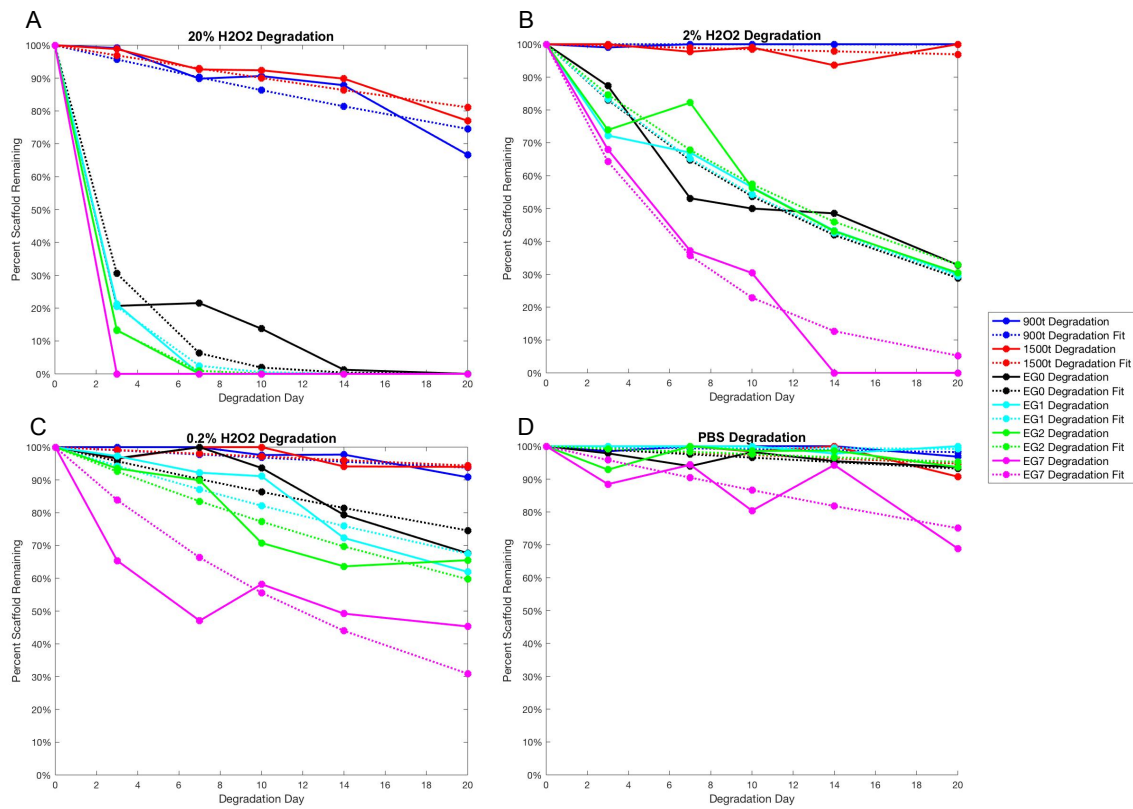
Figure A1. MATLAB generated graphs of degradation kinetics for (A) 20%/0.1M H_2O_2/CoCl$_2$, (B) 2%/0.01M H_2O_2/CoCl$_2$, (C) 0.2%/0.001M H_2O_2/CoCl$_2$, and (C) PBS. Solid lines represent measured data and dotted lines represent MATLAB generated best-fit curves.

APPENDIX B: Chapter 4 Supplementary Information

Polymer	MW of monomer	MW of polymer	MW of repeating unit	MW of end group	Repeating Unit
EG0	122.25	2000	162.06	199.38	11.11
EG1	138.25	2000	193.35	226.37	9.17
EG2	182.3	2000	222.38	270.42	7.78
EG7	400	2000	651.38	400	2.46

Table B1. Repeating unit (TK per monomer) for each PTK polymers based on 2000 Da molecular weight.

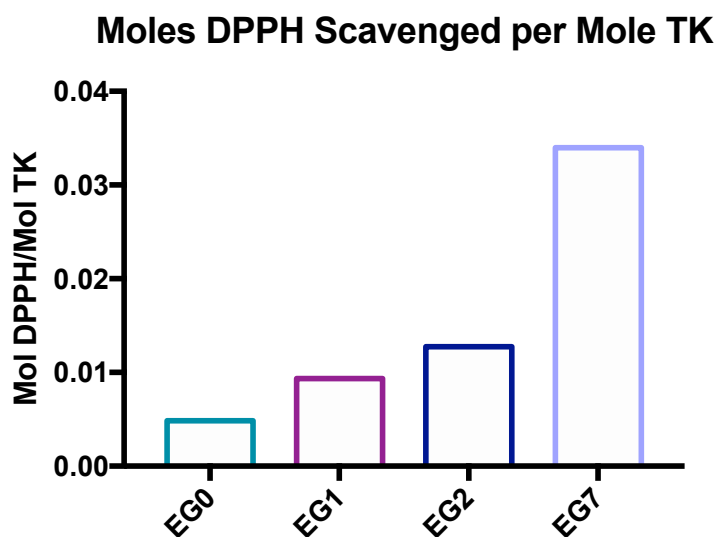## Moles DPPH Scavenged per Mole TK

Figure B1. Moles of DPPH scavenged per mole of thioketal bonds present in each PTK monomer. Values extrapolated from standard curve using repeating unit values found in **table B1.**

Polymer	mg/mL Polyol
900t	0.5
1500t	0.5
EG0	0.34
EG1	0.42
EG2	0.48
EG7	1.4

Table B2. Polyol mass concentration used for cytoprotection experiments. Polyols were matched based on moles of TK units available for ROS scavenging.
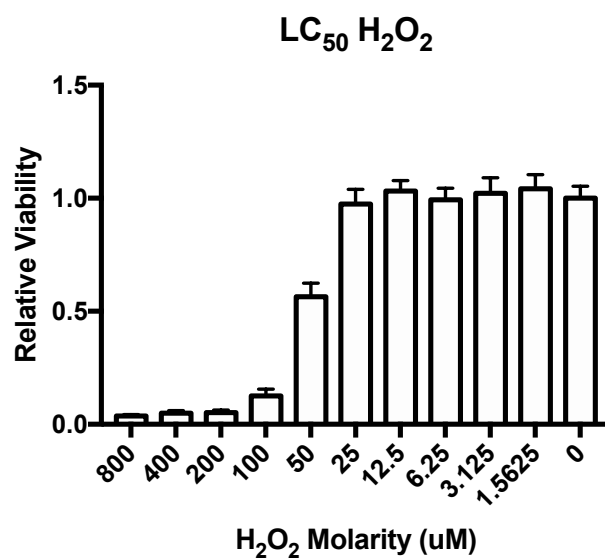
Figure B2. LC$_{50}$ analysis for NIH 3T3 cells treated with hydrogen peroxide used to determine hydrogen peroxide concentrations for cytoprotection studies. Relative viability was measured at 24 hours using Cell Titer-Glo Bioluminescence assay in reference to a no treatment control.